Elliptic flow of charged hadrons in Au+Au collisions at $\sqrt{s_{NN}} = 200$ GeV: Detailed comparison of PHENIX and STAR results

A. Taranenko , Roy A. Lacey, Stanislav Salnikov

Chemistry Dept.
Stony Brook University,
Stony Brook, NY 11794-3400

Abstract

We present the detailed comparison of PHENIX/STAR results of elliptic flow (v_2) measurements for charged hadrons emitted from Au+Au collisions at $\sqrt{s_{NN}}$ as a function of collision centrality and the transverse momentum p_T of the emitted hadron. As the reference for such comparison we are using recent Run 2007 PHENIX flow measurements of charged hadrons with respect to the MPC ($3.1 < |\eta| < 3.7$) and RXN combined ($1.0 < |\eta| < 2.8$) event planes.

Contents

1 Introduction **2**

2 STAR published v_2 data used for comparison **8**

3 Analysis **13**
3.1 Run selection 13
3.2 Event and track selection 14
3.3 Comparison with preliminary results 17
3.4 Results for Preliminary Request 18

4 Comparison with different STAR flow methods **22**
4.1 Standard Event Plane Method $v_2\{\mathrm{EP}\}$ 22
4.2 Modified Event Plane Method $v_2\{\mathrm{EP}_2\}$ 24
4.3 Modified Two-Particle Correlation Method: $v_2\{v_2\text{-pp}\}$ 27
4.4 Two-Particle Cumulant Method: $v_2\{2\}$ 28
4.5 Four-Particle Cumulant Method: $v_2\{4\}$ 29
4.6 Lee-Yang Zero method: $v_2\{\mathrm{LYZ}\}$ 30

5 Detailed p_T/centrality comparison for v_2 between PHENIX/STAR **31**

6 Comparison with PHOBOS v_2(p_T,centrality) results **38**

7 Deta tables with $v_2(p_T, centrality\ )$ results **40**

1 Introduction

After ten years of extensive studies of elliptic flow at RHIC there is a clear luck of detailed systematic comparisons between results of differential elliptic flow measurements performed by different collobarations. One can find only few examples of such comparisons in the published articles and sometimes they are not fully consistent.
Comparison between STAR and PHOBOS v_2 data

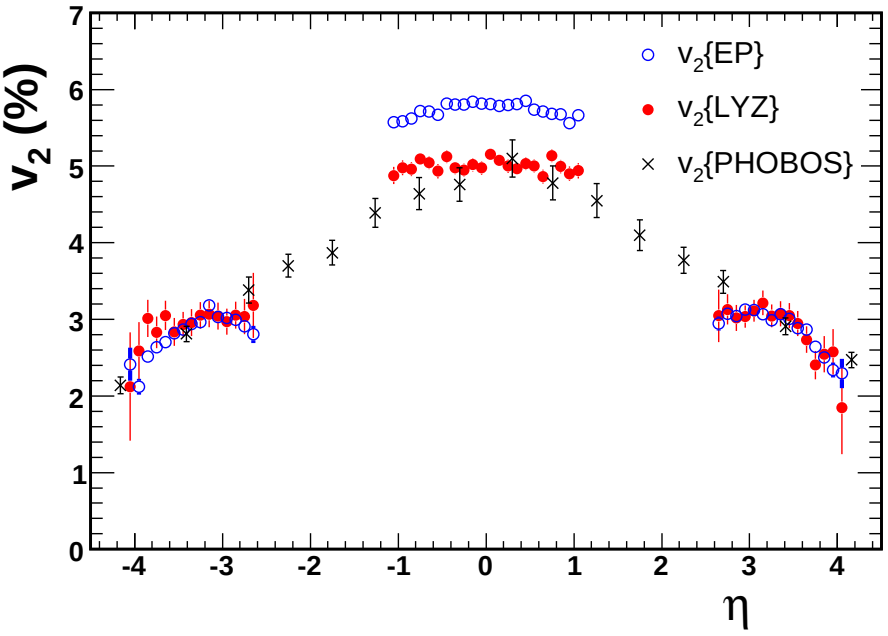

Figure 1: Pseudorapidity η dependence of integral eliiptic flow of charged hadrons from 10-40% central Au+Au collisions at $\sqrt{s_{NN}}$ = 200-GeV. STAR v_2 data for charged hadrons [4] from the Lee-Yang zero product generating function (solid circles) and from the event plane method (open circles), as a function of pseudorapidity. Both sets of data have been averaged over p_T from 0.15 to 2.0 GeV/c. For comparison, the PHOBOS data (10-40%) [6] (crosses) are also shown. The error bars are shown only for the statistical uncertainties. The plot is taken from [4]

Comparison of the measurements of the pseudorapidity η dependence of integral eliiptic flow of charged hadrons between STAR and PHOBOS [2, 4]. The comparison was made for 10-40% central Au+Au collisions at $\sqrt{s_{NN}}$ = 200-GeV. The results depends on the method of flow measurements used by STAR collaboration. At midrapidity $|\eta| < 1$, PHOBOS v_2 data [6] are found to be by 15% smaller than STAR v_2 data obtained using measurements with respect to event plane from STAR central TPC. But, they are consistent with STAR Lee-Yang Zeros v_2 data [4], see Fig. 1 . For forward rapidities all STAR methods look in agreement between each other and PHOBOS data [4]. Another comparison between STAR [2] and PHOBOS [5] was done for

p_T dependence of elliptic flow of charged hadrons emitted at midrapidity from (0-50%) central Au+Au collisions at $\sqrt{s_{NN}} = 200$-GeV [2], see Fig. 2. In this case the STAR v_2 data were obtained from using measurements with respect to event plane from STAR central TPC. The ratio plot shows that this time both event plane v_2 measurements are indeed in a good agreement.

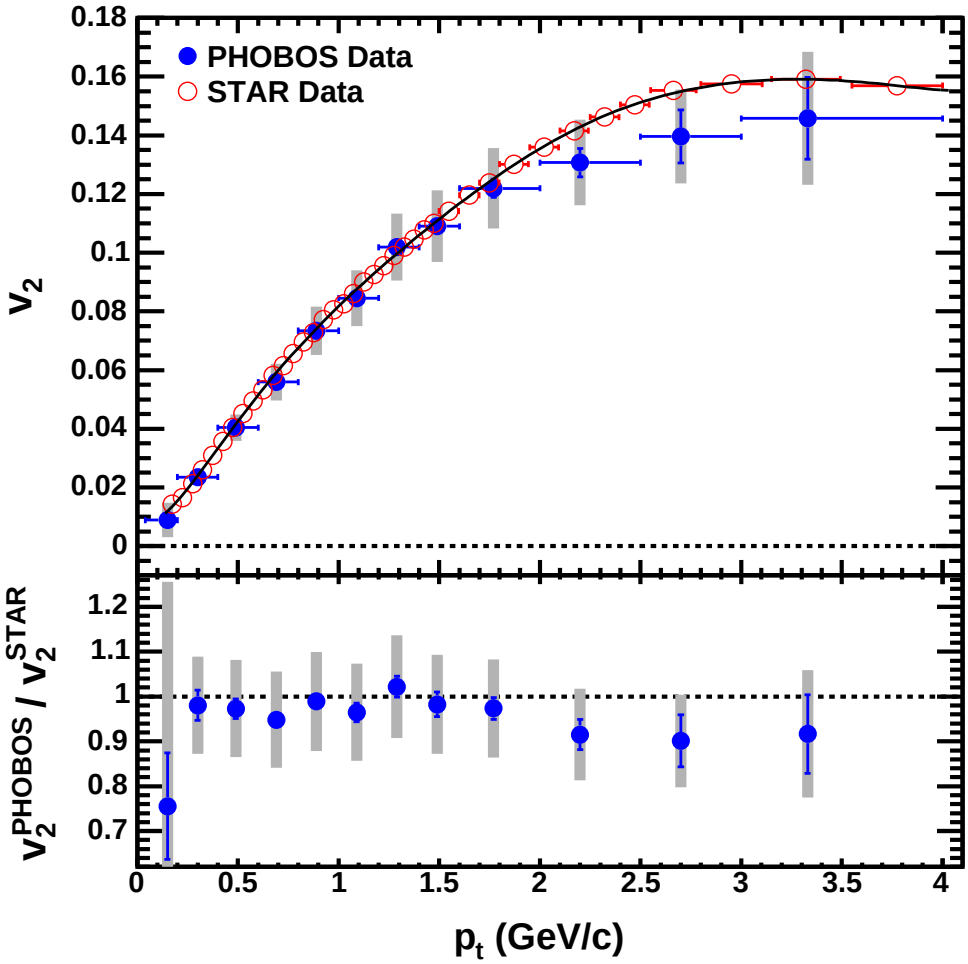

Figure 2: p_T dependence of elliptic flow of charged from 0-50% central Au+Au collisions at $\sqrt{s_{NN}} = 200$-GeV. STAR v_2 data (open circles) are from standard event plane method using central TPC [2]. PHOBOS v_2 data (solid circles) are for charged hadrons with ($0 < \eta < 1.5$) measured with respect to event plane ($2.05 < |\eta| < 3.2$). The line is a polynomial fit to the STAR data. The gray error boxes represent the PHOBOS systematic errors. The bottom panel shows the ratio of the PHOBOS data to the polynomial fit. The plot is taken from [2]

Comparison between PHENIX and STAR PID v_2 data

Comparison of the p_T dependence of elliptic flow for low p_T charged pions, kaons

and (anti-) protons from minimum-bias Au+Au collisions at $\sqrt{s_{NN}}$ = 200-GeV using standard event plane method results from STAR and PHENIX [2]. For event plane method STAR used particles from midrapidity $|\eta| < 0.75$ while the PHENIX used event plane from BBC counters $3.1 < |\eta| < 3.9$. A slightly different conlcusion from the comparison of the minimum-bias data for v_2 of charged pions, kaons and protons from PHENIX and neutral kaons, Lambdas and Cascades from STAR were drawn in [7]. In order for both data sets to follow KE_T/n_q scaling the STAR v_2 values were multiplied by the constant factor 1.1 to account for a small difference between the average centralities for minimum bias events from the two experiments.

Comparison between PHENIX and STAR v_2 of charged hadrons: centrality and p_T dependence

Detailed comparison of p_T dependence of elliptic flow of charged hadrons for different bins in collision centrality between PHENIX and STAR excluding top 0-10% central collisions was performed in [8]. PHENIX v_2 measurements were performed using :
(1) event plane method from two independent sub-detectors at forward ($|\eta| = 3.1$–3.9) v_2(BBC) and beam ($|\eta| > 6.5$) pseudorapidities v_2(ZDC)
(2) two-particle cumulant method $v_2(2)$ extracted using correlations between particles detected at midrapidity $|\eta| <0.35$.
STAR v_2 measurements [used for comparison] were obtained using two-particle $v_2\{2\}$ and four-particle cumulant method $v_2\{4\}$ for 20-60% central Au+Au collisions at $\sqrt{s_{NN}}$ = 200-GeV. For 10-20%, 20-30% and 30-40% central Au+Au collisions STAR v_2 data were obtained by co-called modified event plane method using STAR central TPC [2], labelled $v_2\{\mathrm{EP}_2\}$, : particles within $|\Delta\eta| < 0.5$ around the highest $p_T$particle were excluded for the determination of the modified event plane in order to reduce some of the non-flow effects at high p_T.
Figure Fig. 3 [taken from [8]] shows the p_T dependence of v_2 for charged hadrons from 20-60% central Au+Au collisions. Different symbols corresponds to the data points from PHENIX and STAR. The following canclusions were drawn from this camparison plot:
1) results from two particle cumulant method $v_2\{2\}$ from PHENIX is lower than that from STAR.
2) results from event plane measurements from PHENIX is lower than four particle cumulant results $v_2\{4\}$ from STAR with the following order: $v_2\{\mathrm{BBC}\} > v_2\{\mathrm{ZDC\text{-}SMD}\} > v_2\{4\}$
Figure Fig. 4 shows the p_T dependence of v_2 for charged hadrons for 10-20%, 20-30% and 30-40% central Au+Au collisions. Different symbols corresponds to the PHENIX v_2 data obtained from event plane method [BBC and ZDC/SMD] and STAR $v_2\{\mathrm{EP}_2\}$ values were obtined from the modified event plane method, see above. The following canclusions were drawn from this camparison plot: PHENIX $v_2\{\mathrm{BBC}\}$ agrees well with STAR $v_2\{\mathrm{EP}_2\}$ over the measured $p_T$range, whereas PHENIX $v_2\{\mathrm{ZDC\text{-}SMD}\}$ is generally slightly smaller than $v_2\{\mathrm{EP}_2\}$.
However the comparison plots were presented in terms v_2 plotted as a function of

transverse momentum p_T for both STAR and PHENIX data. As v_2 as a function of p_T is changing magnitude by almost a factor 5-10 starting at 1-3% at low p_T to 9-18% at intermidiate p_T such way of comparison of different set of data does not help to understand the presize value of the difference. The presentation of different data sets in terms of their ratio plotted as a function of p_T/centrality for a possible narow bin in centrality/p_T helps much better to unrderstand the differences on a quantative level and possible origin of it.

In the present work we will provide the detailed comparison of PHENIX/STAR results of elliptic flow (v_2) measurements for charged hadrons emitted from Au+Au collisions at $\sqrt{s_{NN}}$ as a function of collision centrality and the transverse momentum p_T of the emitted hadron. As the reference for such comparison we are using recent Run 2007 PHENIX flow measurements of charged hadrons with respect to the MPC ($3.1 < |\eta| < 3.7$) and RXN combined ($1.0 < |\eta| < 2.8$) event planes. The PHENIX flow measurements of charged hadrons were generated for the same centrality/p_T selections as available published STAR results. They were generated from the same analysis as the charged hadron v_2 results were generated for ppg98 and they are in agreement with preliminary results for ppg98 [1] if one use the same centrality/p_T selections.

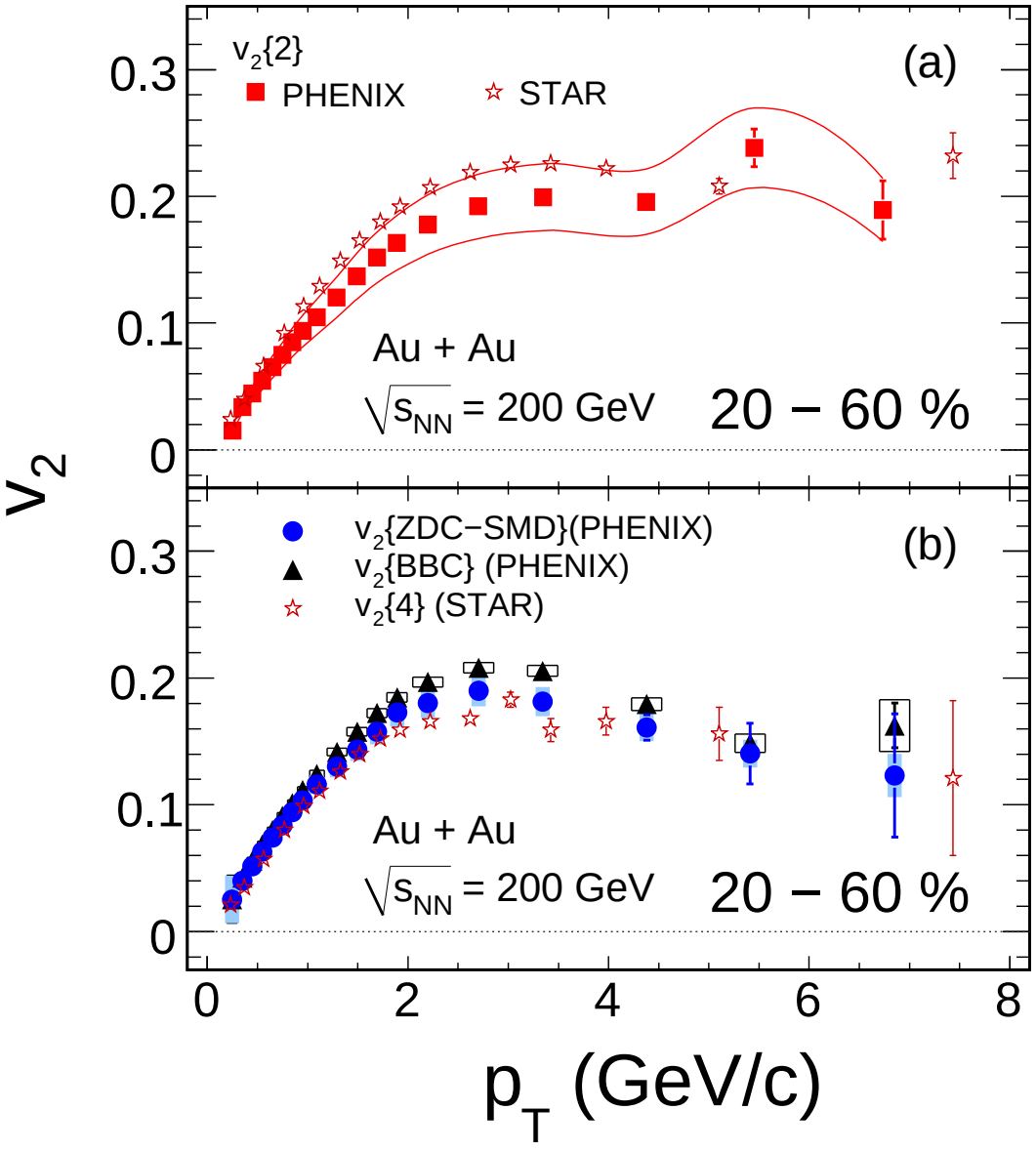

Figure 3: (a) Comparison of charged hadron $v_2\{2\}$ between PHENIX (filled squares) and STAR experiments (open stars) as a function of $p_T$in centrality 20–60%. Solid lines represent the quadratic sum of type B and C systematic errors on the PHENIX $v_2\{2\}$. (b) Comparison of charged hadron v_2 from four-particle cumulant $v_2\{4\}$ at STAR (open stars) with the PHENIX $v_2\{\text{BBC}\}$ (filled triangles) and $v_2\{\text{ZDC-SMD}\}$ (filled circles) as a function of $p_T$in centrality 20–60%. Open boxes and shaded bands represent the quadratic sum of type B and C systematic errors on the $v_2\{\text{BBC}\}$ and $v_2\{\text{ZDC-SMD}\}$, respectively. STAR results are taken from Ref. [3]. The figure is taken from [8]

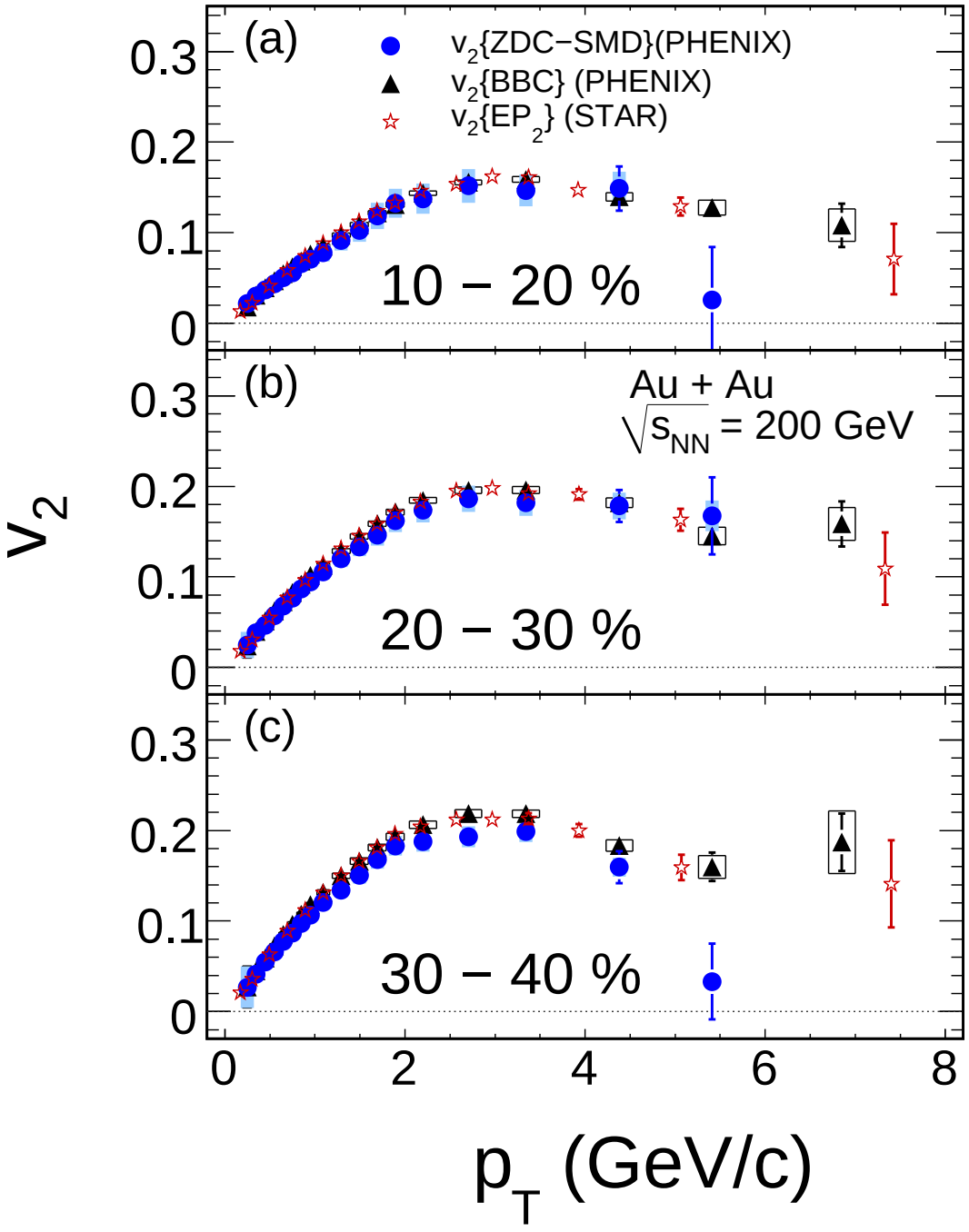

Figure 4: Comparison of the PHENIX $v_2\{\text{BBC}\}$ (filled triangles) and $v_2\{\text{ZDC-SMD}\}$ (filled circles) with the STAR v_2 from modified event plane method (open stars) for charged hadrons [2] as a function of $p_T$in centrality (a) 10–20%, (b) 20–30%, and (c) 30–40%. Open boxes and shaded bands represent the quadratic sum of type B and C systematic errors on $v_2\{\text{BBC}\}$ and $v_2\{\text{ZDC-SMD}\}$, respectively. The figure is taken from [8]

2 STAR published v_2 data used for comparison

In this section we will briefly review and discuss the published STAR v_2 data [3, 2, 4] which will be used later for comparison with PHENIX results.
1) The STAR v_2 data are for charged hadrons from Au+Au collisions at $\sqrt{s_{NN}}$ = 200-GeV. They represent the data sets for Runs: 2002 and 2004. The data points were taken from STAR web page [3, 2, 4]
2) Multiparticle flow methods: The published STAR v_2 data obtained using the multiparticle flow methods like four particle cumulants $v_2\{4\}$ and Lee-Yang Zeros method $v_2\{\text{LYZ}\}$ are available only for a mid-central collisions and broader centrality bins as 10-40% and 20-60%. In order to obtaine reasonable error bars for such methods one really need to deal with large v_2 values and event multiplicity. For example the Lee-Yang Zeros method only works for a sufficient signal-to-noise ratio. Since the signal is v_2 and the noise is proportional to $1/\sqrt{M}$, where M is multiplicity.

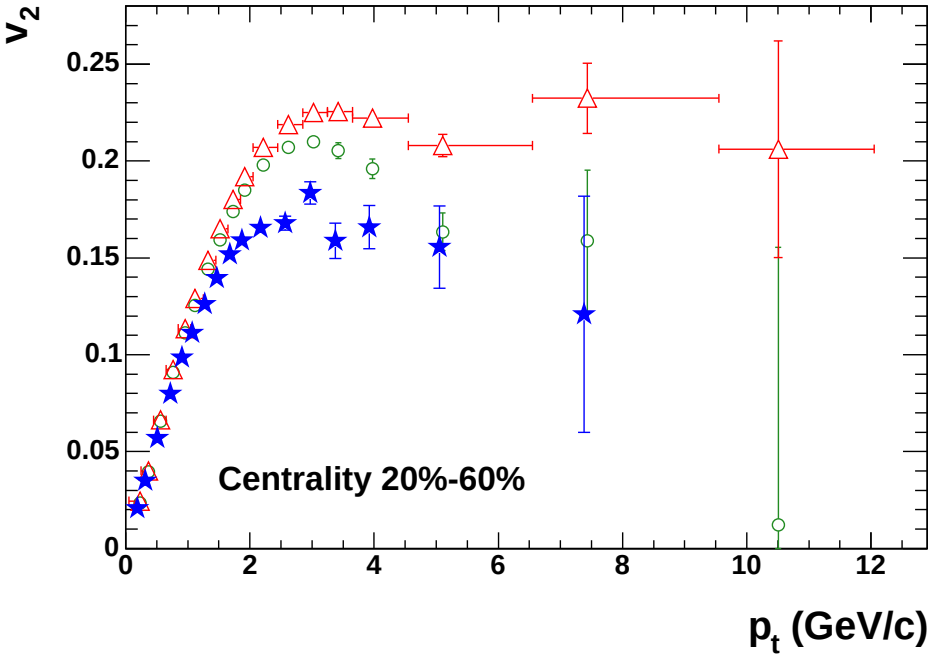

Figure 5: (Color online). STAR results for v_2 of charged particles from 20-60% central Au+Au collisions as a function of transverse momentum p_T from the two-particle cumulant method $v_2\{2\}$ (triangles) and four-particle cumulant method $v_2\{4\}$ (stars). Open circles show the two-particle correlation results after subtracting the correlations measured in p+p collisions $v_2\{\text{v2-pp}\}$. Only statistical errors are shown. Figure is taken from [3]

The parameter $\chi = v_2 \cdot \sqrt{M}$ determines the applicability of the method. The Lee-Yang Zeros method will not work for χ values less than 0.8 , or if the the full event plane resolution is less than 0.6 [9]. For STAR at 200 GeV Au+Au the Lee-Yang Zeros method fails for central collisions because v_2 is small, and for peripheral collisions

because the multiplicity is small [9]
Figure 5 shows the v_2 of charged particles from 20-60% central Au+Au collisions as a function of transverse momentum p_T from the two-particle cumulant method $v_2\{2\}$ (triangles) and four-particle cumulant method $v_2\{4\}$ (stars). Open circles show the two-particle correlation results after subtracting the correlations measured in p+p collisions $v_2\{\text{v2-pp}\}$. On the next Fig. 6 the same data set is presented in form of p_T dependence of the ratios to the $v_2\{2\}$ measured by two particle cumulant method are shown for four particle cumulant method $v_2\{4\}/v_2\{2\}$ (red closed circles) and for two-particle correlation method after subtracting the correlations measured in p+p collisions $v_2\{v_2\text{-pp}\}/v_2\{2\}$ (closed boxes).

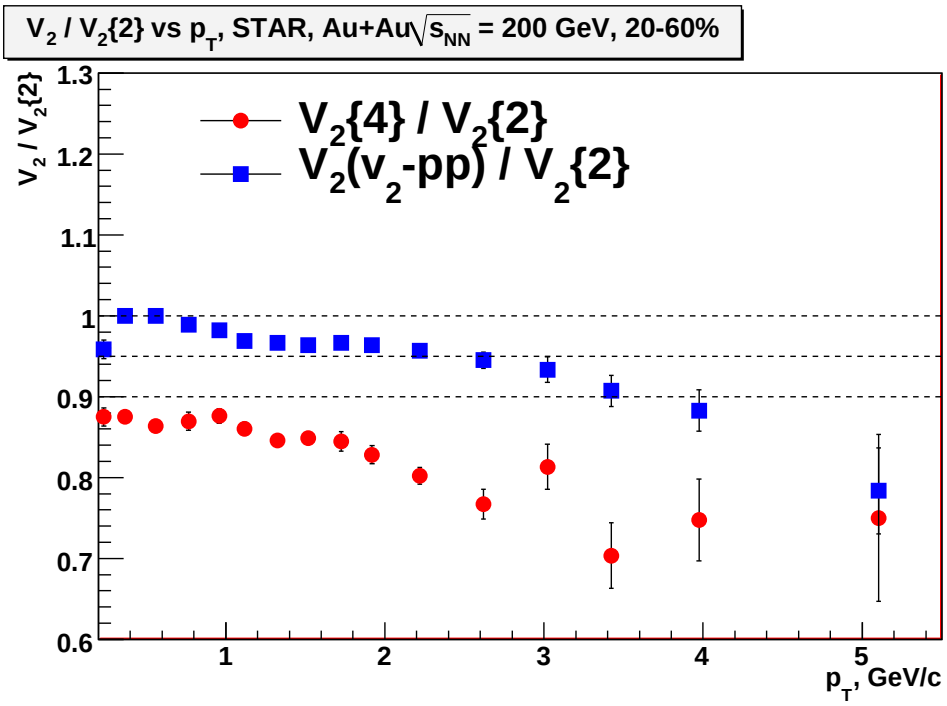

Figure 6: p_T dependence of the ratios to the $v_2\{2\}$ measured by two particle cumulant method are shown for four particle cumulant method $v_2\{4\}/v_2\{2\}$ (red closed circles) and for two-particle correlation method after subtracting the correlations measured in p+p collisions $v_2\{v_2\text{-pp}\}/v_2\{2\}$ (closed boxes). The data represent STAR results for v_2 from 20-60% central Au+Au collisions and taken from [3]

The v_2 obtained using the four-particle cumulant method, $v_2\{4\}$, is up to about 10-25% lower than the value of v_2 obtained from the two-particle cumulant method $v_2\{2\}$ and the difference depends on transversa momentum of the particle, see Fig. 6. The v_2 results obtained by for two-particle correlation method after subtracting the correlations measured in p+p collisions $v_2\{v_2\text{-pp}\}$ are found to be smaller than $v_2\{2\}$, but larger than $v_2\{4\}$ although they looks the same at high p_T. The interpretation of these results by the authors of the STAR paper [3] is that the difference $v_2\{4\}/v_2\{2\}$ could be partially explained by non-flow effects, which should be greatly suppressed in $v_2\{4\}$, and by the fluctuation of v_2 itself. Flow fluctuations contribute to $v_2\{2\}$

and $v_2\{4\}$ with different signs. The true v_2 may lies between $v_2\{4\}$ approximately the average of $v_2\{2\}$ and $v_2\{4\}$ [3]. The next Fig. 7 shows the comparison of the v_2 results obtained standard event plane method $v_2\{\text{EP}\}$ (open circles), 4-particle cumulant method (solid squares) $v_2\{4\}$ and Lee-Yang Zero method (solid circles) with Sum Generating Function $v_2\{\text{LYZ}\}$. The v_2 results are for 10-40% central Au+Au collisions and all methods use the charged particle detected in STAR central TPC ($|\eta| < 1.0$) [4]. The lower panel of Fig. 7 shows the v_2 ratio plots with respect to the $v_2\{\text{EP}\}$ obtained by standard event plane method. The ratio for 4-particle cumulants $v_2\{4\}/v_2\{\text{EP}\}$ decrease with p_T as one would expect for a non-flow contribution from jets at high p_T but, the ratio for Lee-Yang Zero method $v_2\{\text{LYZ}\}/v_2\{\text{EP}\}$ does not change with p_T and this one can hardly be explained by non-flow picture as Lee-Yang Zero method should reduce more non-flow by definition [9].

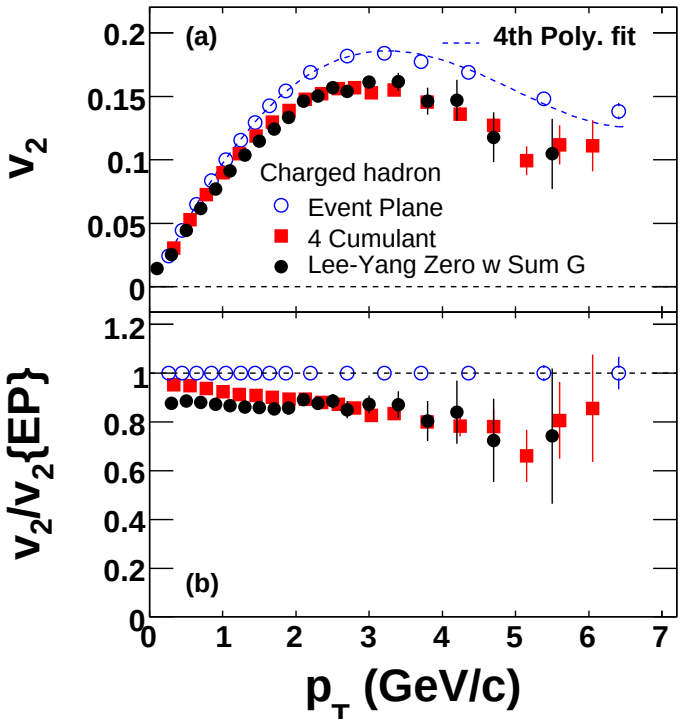

Figure 7: (Color online) (a) v_2 as a function of $p_T$for charged hadrons with $|\eta| < 1.0$ in 10-40% central Au+Au collisions, at $\sqrt{s_{NN}}$= 200 GeV, from the Event-Plane method (open circles), 4-particle cumulant method (solid squares), and Lee-Yang Zero method (solid circles) with Sum Generating Function. (b) The ratios to the polynomial fit to $v_2\{\text{EP}\}$ are shown for $v_2\{4\}/v_2\{\text{EP}\}$ and $v_2\{\text{LYZ}\}/v_2\{\text{EP}\}$ as a function of transverse momentum. The error bars are shown only for the statistical uncertainties. Figure is taken from [4]

3) For the same reason the published results for detailed centrality/p_T dependence for v_2 of charged hadrons in Runs 2002 and 2004 are exist only for the standard event

plane method $v_2\{\text{EP}\}$ and modified event plane $v_2\{EP_2\}$ methods using STAR TPC. Fig. **??** shows p_T for charged hadrons from Au+Au collisions at $\sqrt{s_{NN}}$ = 200-GeV for different centrality bins. The standard reaction plane method $v_2\{\text{EP}\}$ is shown by open symbols and the modified reaction plane method by solid symbols $v_2\{EP_2\}$ [2].

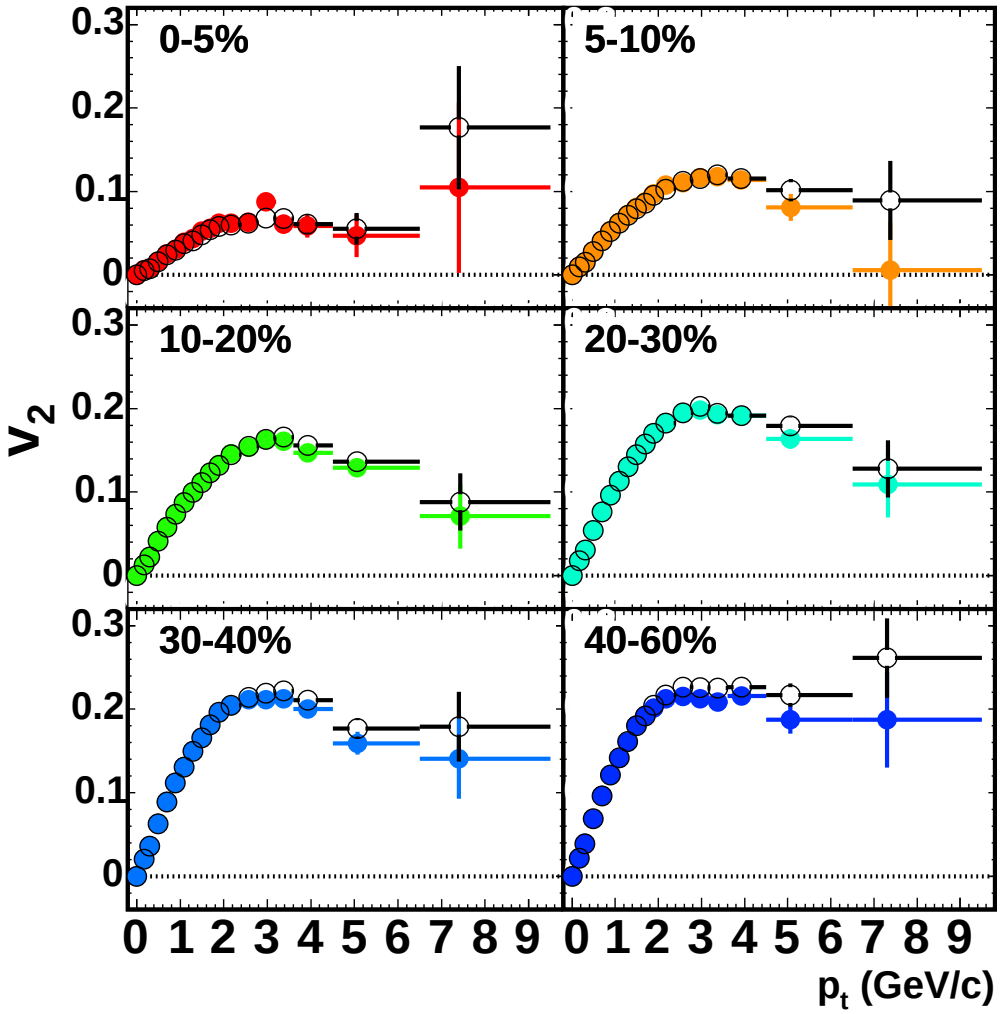

Figure 8: (Color online) STAR results for v_2 vs. p_T for charged hadrons from Au+Au collisions at $\sqrt{s_{NN}}$ = 200-GeV for different centrality bins. The standard reaction plane method $v_2\{\text{EP}\}$ is shown by open symbols and the modified reaction plane method by solid symbols $v_2\{EP_2\}$. The figure is taken from [2]

The modified event plane method $EP_2\}$ excludes particles within $|\eta|$ ¡ 0.5 around the highest p_T particle. For both methods v_2 rises linearly up to p_T = 1 GeV/c and then deviates from a linear rise and saturates for p_T ¿ 3GeV/c for all centralities. The v_2 ratio plots $v_2\{EP\}/v_2\{EP_2\}$ are presented in Fig **??** as a function of transverse momentum p_T. At low transverse momenta ($p_T < 2GeV/c$), the v_2 values are very similar for both methods. At higher transverse momenta, v_2 is systematically larger for the standard reaction plane method $\{EP\}$. For more peripheral collisions this effect is larger, and it also begins at lower p_T. This is very similar to the observations

from the comparison of PHENIX $v_2\{2\}$ for $|\eta| < 0.35$ and $v_2\{\text{BBC}\}$ [8]. This maybe an indication that ever such small rapidity gap used in the STAR modified reaction plane method seems to eliminate at least some of the non-flow effects due to jet at high transverse momenta (up to 15-20% at p_T = 5-6 GeV/c in the most peripheral collisions [2].

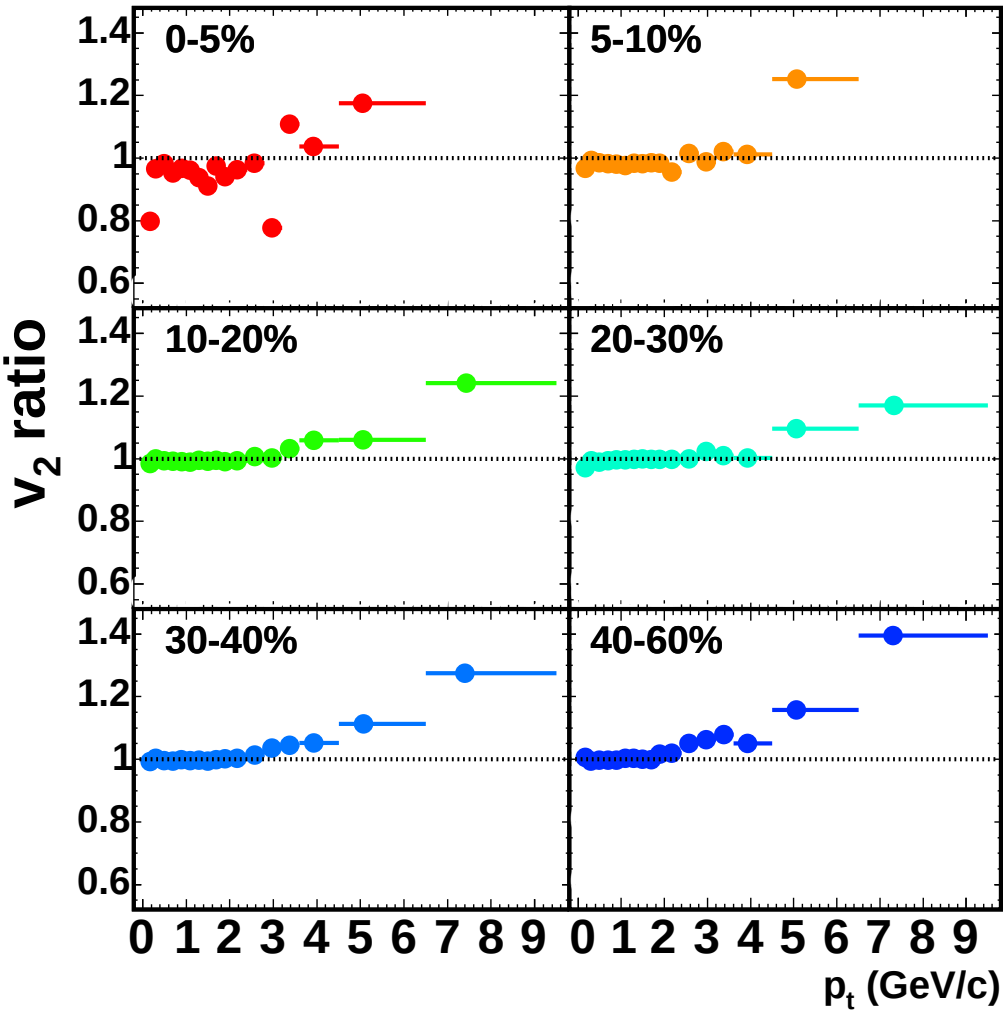

Figure 9: (Color online) STAR results for v_2 for the standard reaction plane method $v_2\{EP\}$ divided by v_2 for the modified reaction plane method $v_2\{EP_2\}$ vs. p_T for charged hadrons in different centrality bins. Error bars are not shown as the same data set is used for both methods. The figure is taken from [2]

3 Analysis

From the previous section we learn that for detailed and compeling comparison with present published STAR v_2 data [2, 3, 4] one need to have PHENIX $v_2 = f(p_T)$ data for the following centrality selection: 0-5%, 5-10%, 10-20%, 20-30%, 30-40%, 40-50% , 40-60%, 10-40% and 20-60%. For comparison with STAR data we are going to use v_2 values for charged hadrons measured with respect to the to the MPC ($3.1 < |\eta| < 3.9$) and RXN combined ($1.0 < |\eta| < 2.8$) event planes. In principle the v_2 values for the these centrality selections can be generated in one step from the preliminary $v_2(p_T$, centrality 5% bins) results used for ppg98 [obtained from TAXI 131 output] by standard averaging procedure. However, we repeated the ppg98 analysis using recent TAXI 170 output which include updated Centrality Calibrator, which was updated after TAXI 131. We also increased the number of p_T bins which help to provide better comparison with STAR published data. The analysis details can be found in the analysis note AN 760.

3.1 Run selection

Only full field runs were analyzed; they include both the (+-) and the (-+) field configurations. In what follows, we give a summary of the criteria for identifying "bad" runs, as well as a list of the runs so rejected;

- Zero field runs (7) : 229545, 231156, 236137, 238530, 238531, 238971, 239312
- (++) field runs (15) : 235889, 235890, 235891, 235892, 235893, 235894, 235895, 235900, 235901, 235902, 236004, 236005, 236007, 236008, 236009
- Converter runs (9) : 238682, 238683, 238684, 238698, 238843, 238845, 238846, 238847, 238848
- Bad centrality runs: 231158
- Runs with a limited number of events (<500 k: 12.423 M events in total): 228640, 228645, 229701, 229799, 229810, 230109, 230163, 230175, 230367, 230557, 231720, 231723, 231770, 233172, 233284, 234449, 234457, 234682, 235366, 235397, 238143, 238171, 239612, 239834, 239914, 240048, 240055, 240116
- Runs which starts from 228*** were not used as they found to be bad for v_2 measurements using BBC, RXN IN and RXN combined event planes: non-flatness of event plane and lower values for average integral elliptic flow, see below.
- Runs which are bad for MPC event plane: 229308, 229310, 229312, 229656, 229793, 229796, 229800, 231155, 231216, 231218, 231221, 235223, 235691, 229309, 229311, 229492, 229790, 229794, 229799, 231154, 231211, 231217, 231219, 233172, 235656, 240115.
- Runs which are bad for RXN event plane: used run list from QA studies of Eric Richardson [10].

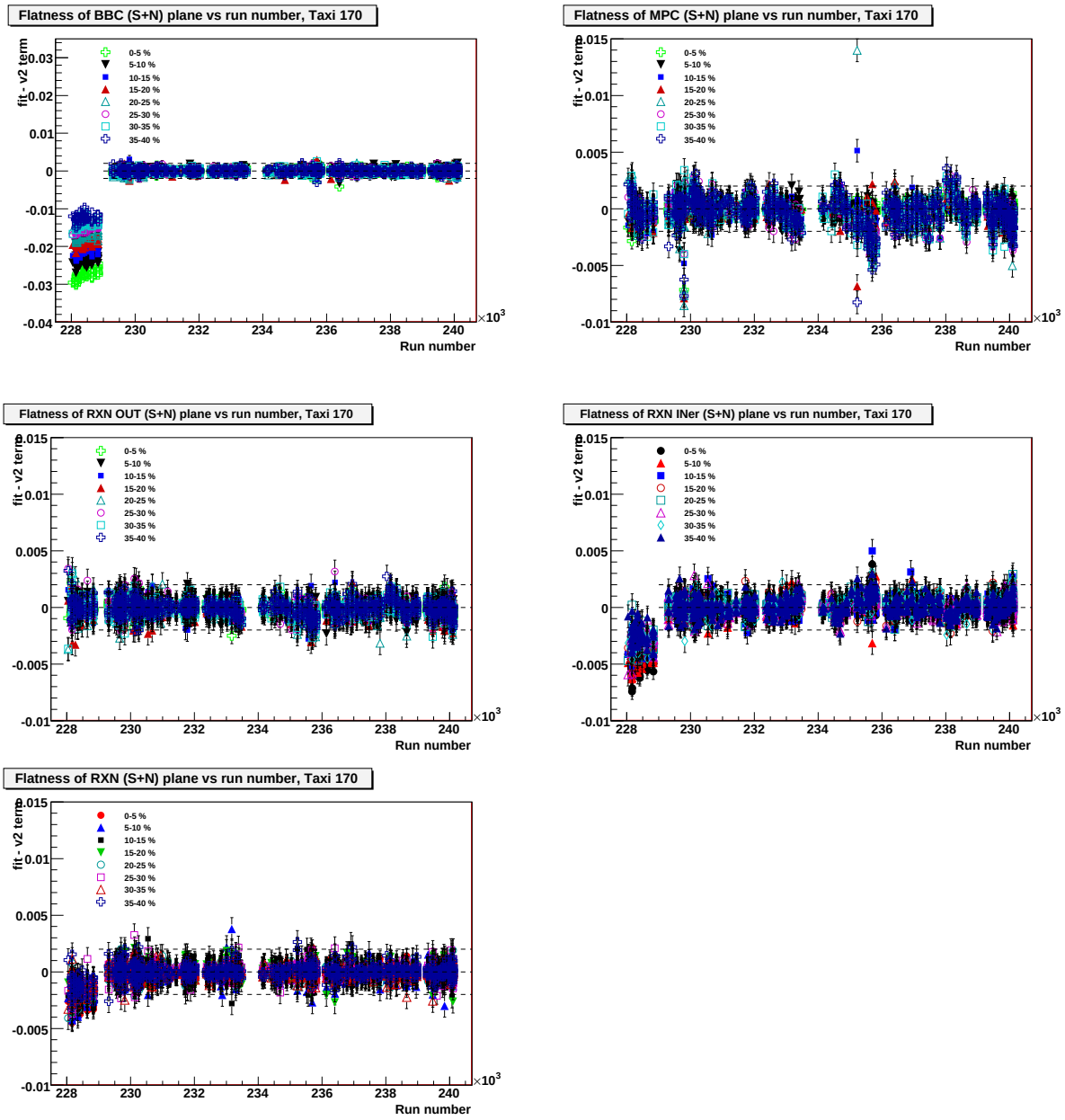

Figure 10: Flatness of the event plane [result of the fit by second Fourier coeff] as a function fo the run number for BBC, MPC , INN, OUT and RXN combined event planes.

3.2 Event and track selection

Event and track selection are the same as used for ppg98 results and listed below:
Event selection:

- Centrality range: 0-60%
- | bbcz | < 30 cm - BBC vertex cut (PHGlobal::getBbcZVertex())

- Use combined (BBC, MPC, RXN combined, RXN Inner and RXN outer parts) south and north eventplane.

Track selection:

- Momentum cut: 0.3-8 GeV/c
- DCH Track Quality: 31 or 63
- | zed | < 75 cm
- 2 σ "radial" matching cut on PC3 + 2 σ "radial" matching cut on EMC
- For high p_T tracks ($p_T > 4GeV$) we used the cut E/p>0.1 to suppress residual background.

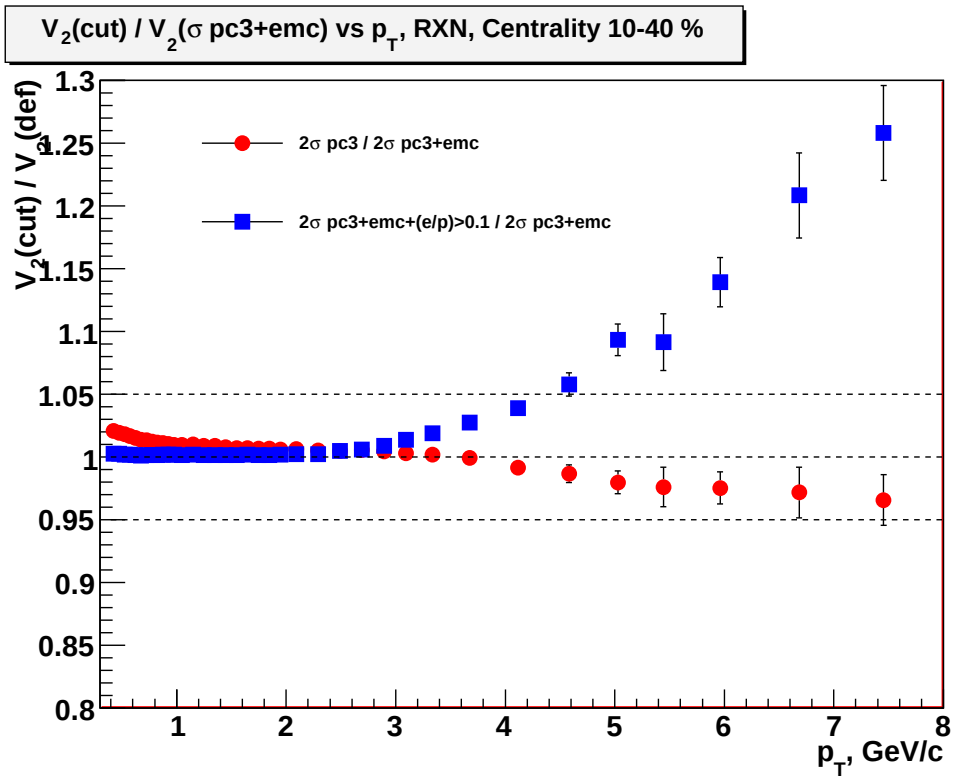

Figure 11: p_T dependence of the ratio v_2 for charged hadrons for several cuts for track selection to v_2 for charged hadrons measured with: 2 σ "radial" matching cut on PC3 + 2 σ "radial" matching cut on EMC. Results for 10-40% central collisions and RXN detector

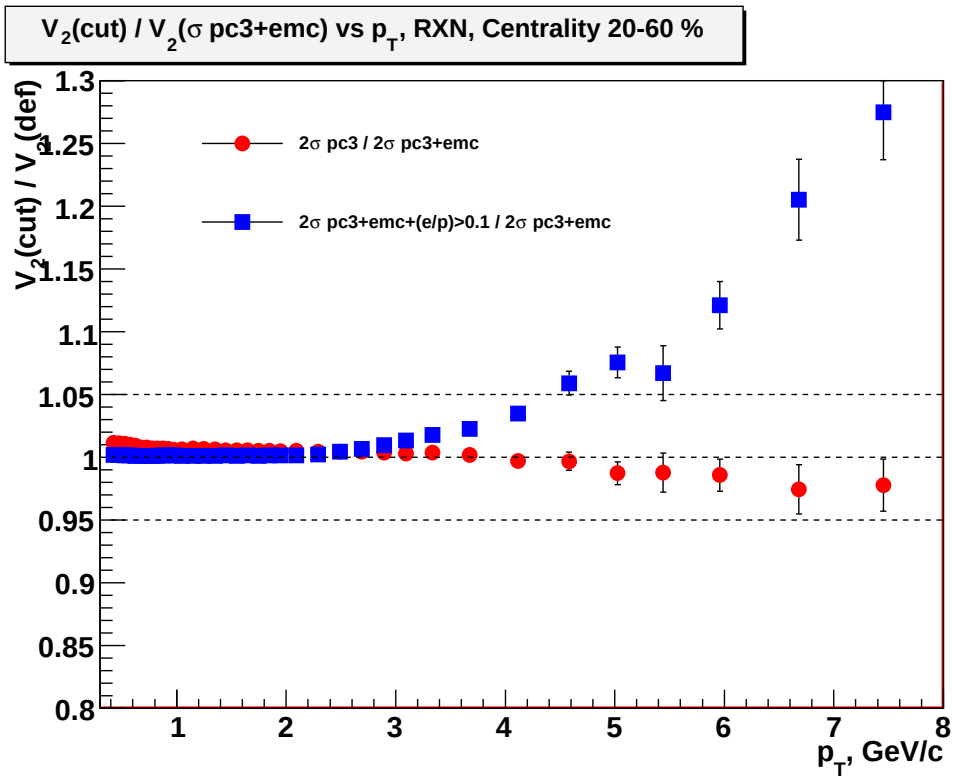

Figure 12: p_T dependence of the ratio v_2 for charged hadrons for several cuts for track selection to v_2 for charged hadrons measured with: 2 σ "radial" matching cut on PC3 + 2 σ "radial" matching cut on EMC. Results for 20-60% central collisions and RXN detector

3.3 Comparison with preliminary results

Fig. 13 shows the N_{part} dependence of the ratio of integral v_2 for charged hadrons measured using the new TAXI 170 output to preliminary v_2 results obtained from TAXI 131. The results are presented for different p_T bins and different event planes as indicated. The ratio plots clearly tell that the differences between new v_2 results and the preliminary ones are less than 1%.

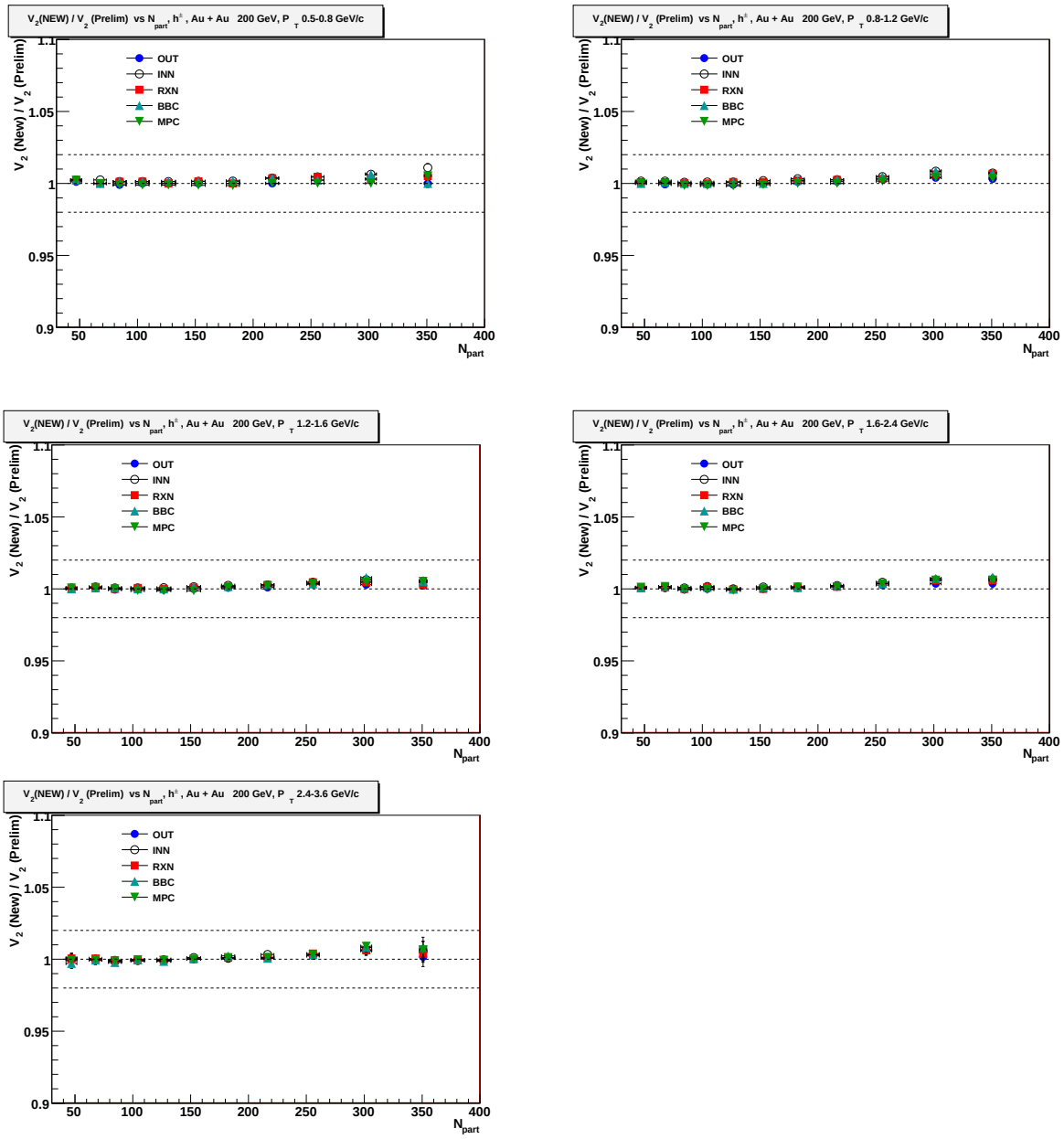

Figure 13: N_{part} dependence of the ratio of integral v_2 for charged hadrons measured using the new TAXI 170 output to preliminary v_2 results obtained from TAXI 131. The results are presented for different p_T bins and different event planes as indicated.

3.4 Results for Preliminary Request

The following $v_2(\ p_T, centrality\ )$ plots are requested for status PHENIX preliminary. The data points are presented in the Appendix of analysis note. The present data set allow the detailed comparison with differential v_2 measurements of charged hadrons from Au+Au collisions at 200 GeV performed by STAR and PHOBOS collaborations at RHIC.

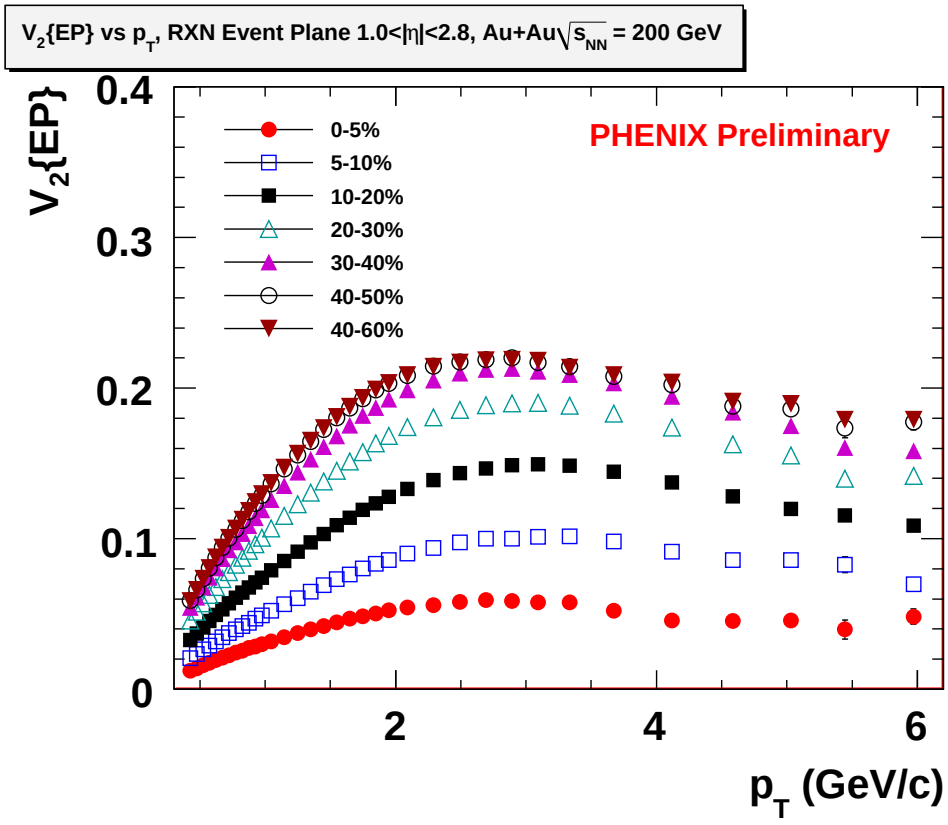

Figure 14: p_T dependence v_2 for charged hadrons from Au+Au collisions at 200 GeV for different bins in collision centrality. The v_2 values were obtained by standard event plane method $v_2\{\mathrm{EP}\}$ using RXN detector $(1.0 < |\eta| < 2.8)$

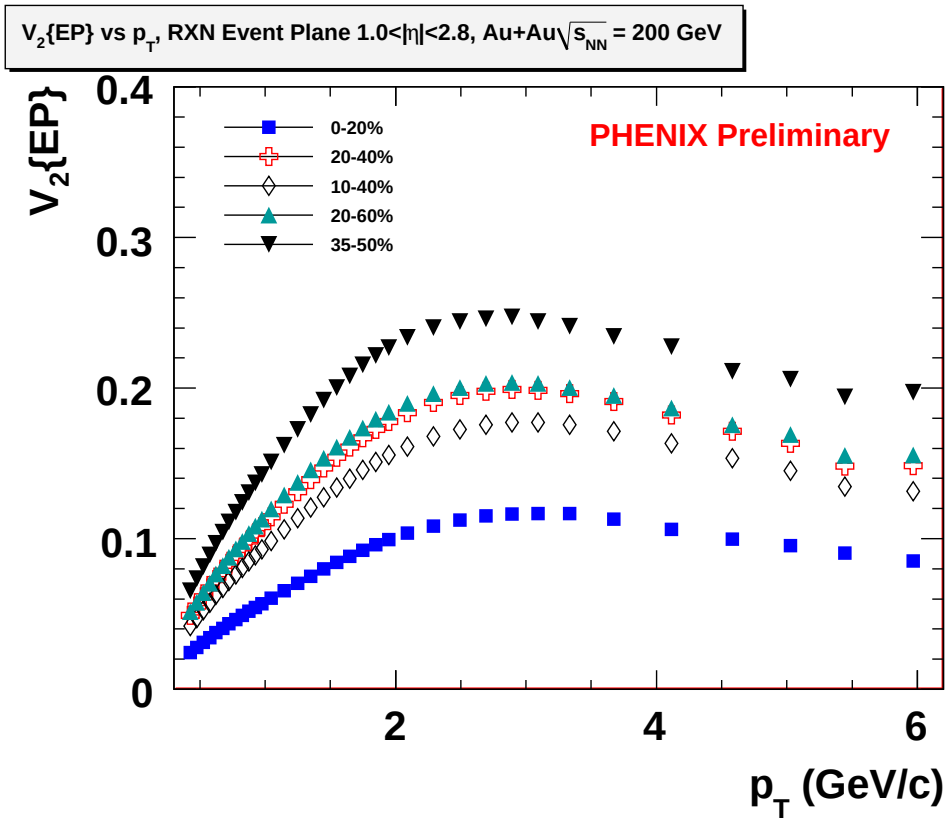

Figure 15: p_T dependence v_2 for charged hadrons from Au+Au collisions at 200 GeV for different bins in collision centrality. The v_2 values were obtained by standard event plane method $v_2\{\mathrm{EP}\}$ using RXN detector ($1.0 < |\eta| < 2.8$)

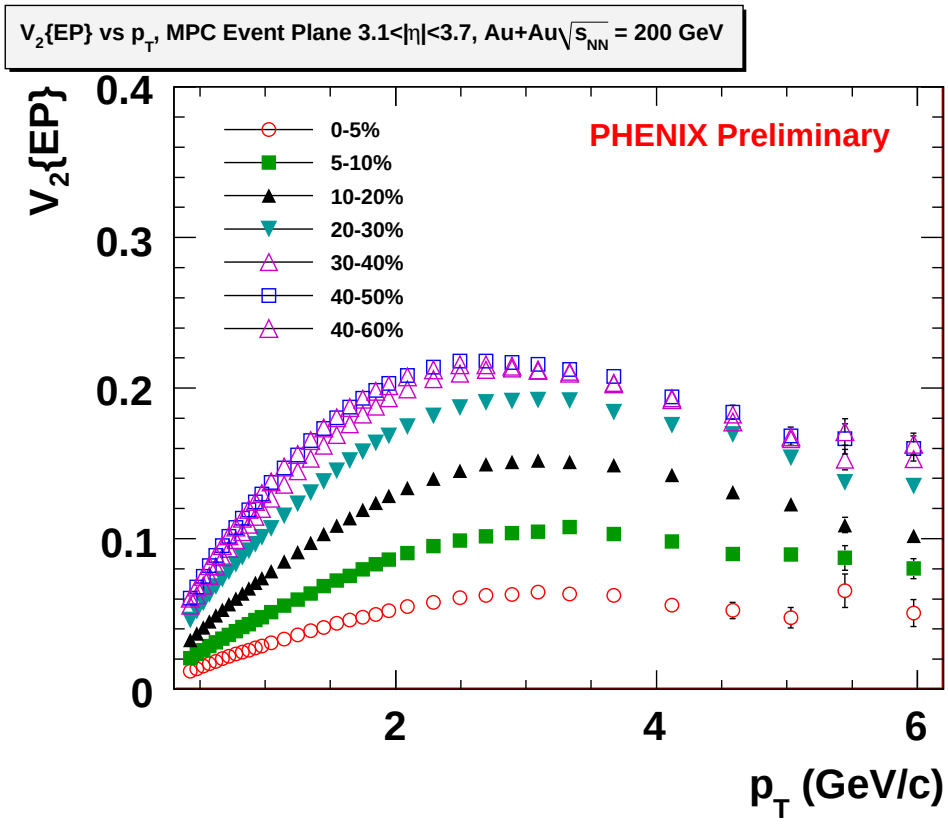

Figure 16: p_T dependence v_2 for charged hadrons from Au+Au collisions at 200 GeV for different bins in collision centrality. The v_2 values were obtained by standard event plane method $v_2\{\mathrm{EP}\}$ using MPC detector ($3.1 < |\eta| < 3.7$)

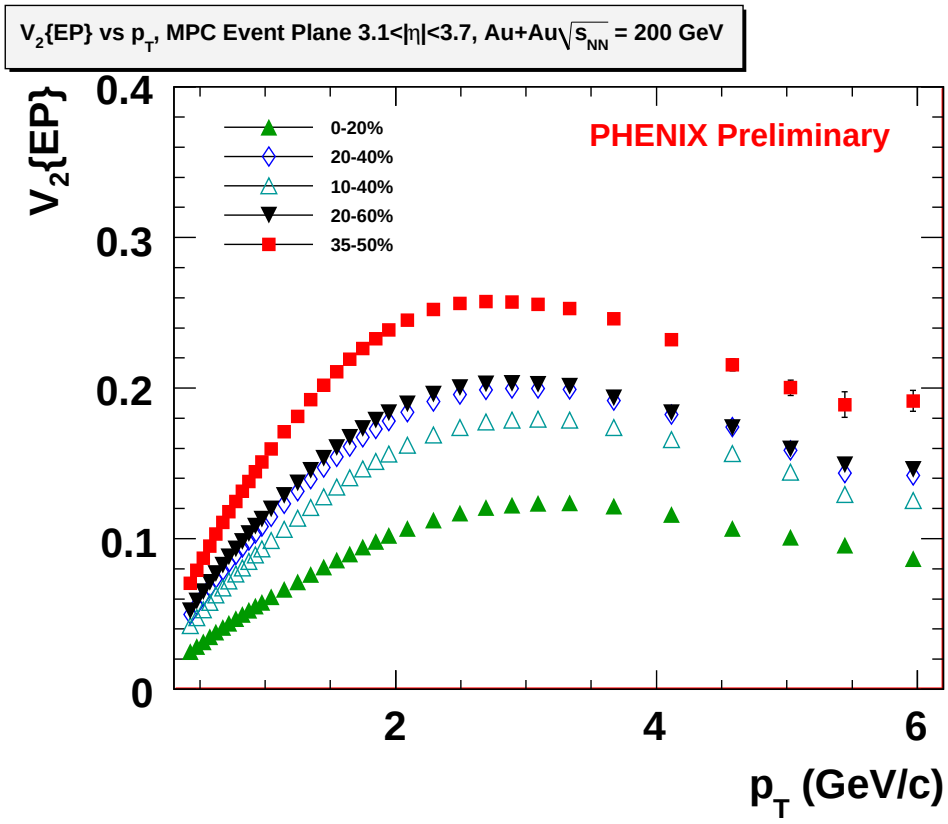

Figure 17: p_T dependence v_2 for charged hadrons from Au+Au collisions at 200 GeV for different bins in collision centrality. The v_2 values were obtained by standard event plane method $v_2\{\mathrm{EP}\}$ using MPC detector ($3.1 < |\eta| < 3.7$)

4 Comparison with different STAR flow methods

In this section we provide detailed comparison of v_2 of charged hadrons from 10-40% and 20-60% mid-central Au+Au collisions and measured with respect to the MPC ($3.1 < |\eta| < 3.7$) and RXN combined ($1.0 < |\eta| < 2.8$) event planes. Only for mid-central collisions one has full set of the published differential STAR v_2 results from Run 2002 and Run 2004 for the reasons explained in the STAR v_2 methods section.

Two-particle STAR flow methods:

- $v_2\{\text{EP}\}$ - standard event plane method ($|\eta| < 1.0$)
- $v_2\{EP_2\}$ - modified event plane method where particles within $|\Delta\eta| < 0.5$ around the highest $p_T$particle were excluded for the determination of the modified event plane in order to reduce some of the non-flow effects at high p_T.
- $v_2\{2\}$ - two-particle cumulant method
- $v_2\{v_2\text{-pp}\}$ - two-particle correlation method with subtraction the correlations measured in p+p collisions.

Multiparticle STAR flow methods:

- $v_2\{4\}$ - four-particle cumulant method
- $v_2\{\text{LYZ}\}$ - Lee-Yang Zero method

4.1 Standard Event Plane Method $v_2\{\text{EP}\}$

Lets start from the comparison with STAR v_2 results obtained by standard event plane method $v_2\{\text{EP}\}$. The technique is very similar to our v_2 measuremments and the difference only is that one use particles at midrapidity region of STAR central TPC ($|\eta| < 1.0$) and one need to be very careful with autocorrelation effects. Figure 18 shows the p_T dependence of the ratio of STAR v_2 values [4] obtained by standard event plane method $v_2\{\text{EP}\}$ to the PHENIX v_2 values obtained by event plane method using event plane from MPC ($3.1 < |\eta| < 3.7$) [closed boxes] and RXN detector ($1.0 < |\eta| < 2.8$) [close triangles]. The comparison is made for v_2 of charged hadrons from 20-30% and 40-60% central Au+Au collisions at$\sqrt{s_{NN}}$ = 200-GeV. As one can see that for these particular centrality bins the difference between STAR/PHENIX v_2 values is less than 2-5% below $p_T \simeq$2.5 GeV/c. At higher transverse momenta, STAR v_2 is systematically larger than the PHENIX v_2 and the ratio is tends to grow with p_T reaching the value of 20% at $p_T \simeq$5.5 GeV/c, see Fig 18. The difference in v_2 values at higher p_T can be attributed to non-flow effects due to di-jets which are mostly supressed by rapidity gaps in case of PHENIX v_2 measurements [11].

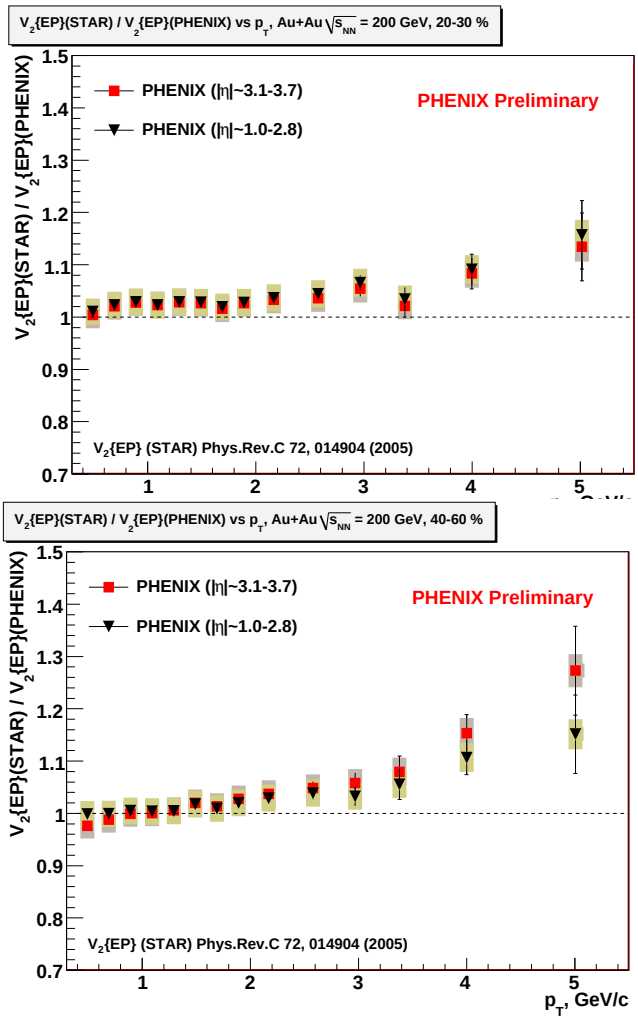

Figure 18: Upper panel: p_T dependence of the ratio of STAR v_2 values obtained by standard event plane method $v_2\{\mathrm{EP}\}$ using central TPC ($|\eta| < 1.0$) to the PHENIX v_2 values obtained by event plane method using MPC/RXN event planes for 20-30% central Au+Au collisions. Lower panel: p_T dependence of the ratio of STAR v_2 values obtained by standard event plane method $v_2\{\mathrm{EP}_2\}$ to the same PHENIX v_2 values for 40-60% central Au+Au collisions. The STAR v_2 data are taken from [2]

4.2 Modified Event Plane Method $v_2\{EP_2\}$

Lets put some small rapidity gap and look on the STAR v_2 data obtained using the modified event plane method $v_2\{EP_2\}$ where particles within $|\Delta\eta| < 0.5$ around the highest $p_T$particle were excluded for the determination of the modified event plane [2]. As there is no STAR v_2 data obtained using the modified event plane method for 10-40% central Au+Au collisions we will use other centrality bins for which both v_2 results from standard and modified event plane method are available [2].

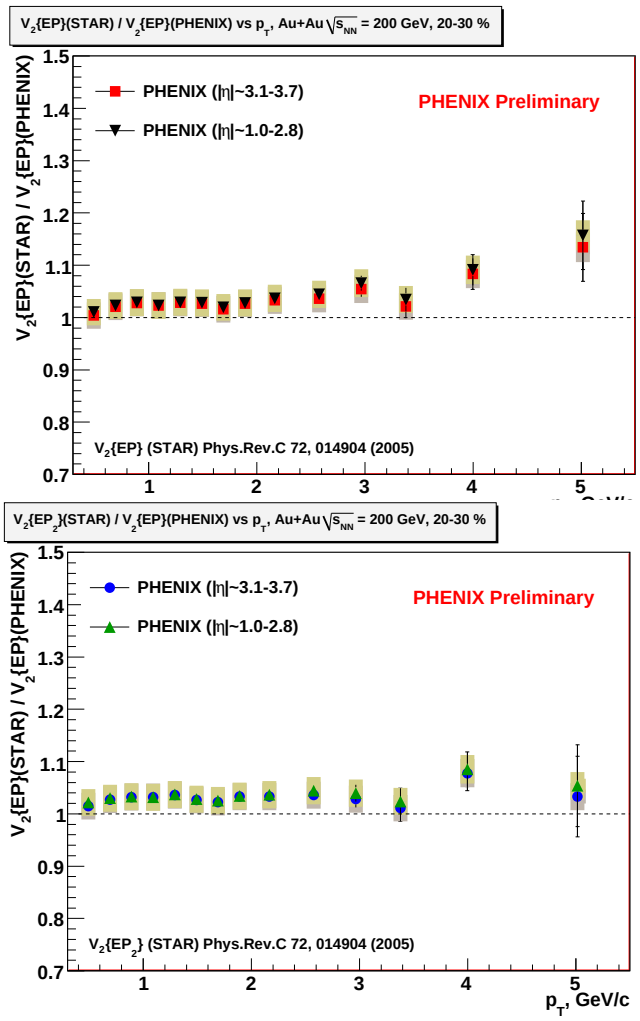

Figure 19: Upper panel: p_T dependence of the ratio of STAR v_2 values obtained by standard event plane method $v_2\{\text{EP}\}$ using central TPC ($|\eta| < 1.0$) to the PHENIX v_2 values obtained by event plane method using MPC/RXN event planes for 20-30% central Au+Au collisions. Lower panel: p_T dependence of the ratio of STAR v_2 values obtained by modified event plane method $v_2\{\text{EP}_2\}$ to the same PHENIX v_2 values. The STAR v_2 data are taken from [2]

The upper panels of Figures 19- 21 show the p_T dependence of the ratio of STAR v_2 values obtained by standard event plane method $v_2\{\text{EP}\}$ to the PHENIX v_2 val-

ues obtained by event plane method using MPC/RXN event planes for three bins in collision centrality: 20-30%, 30-40% and 40-60%. The trends are very similar as for 10-40% central Au+Au collisions plotted in Fig. 18. The lower panels of Figures 19- 21 show the same ratios but in this case the STAR v_2 data were obtained using modified event plane method $v_2\{\mathrm{EP}_2\}$. The difference between STAR/PHENIX v_2 at high p_T is getting much smaller for STAR modified event plane $v_2\{\mathrm{EP}_2\}$ data, but still persist on the level of 10-15% at $p_T \simeq 5.5$ GeV/c for mid-central collisions.

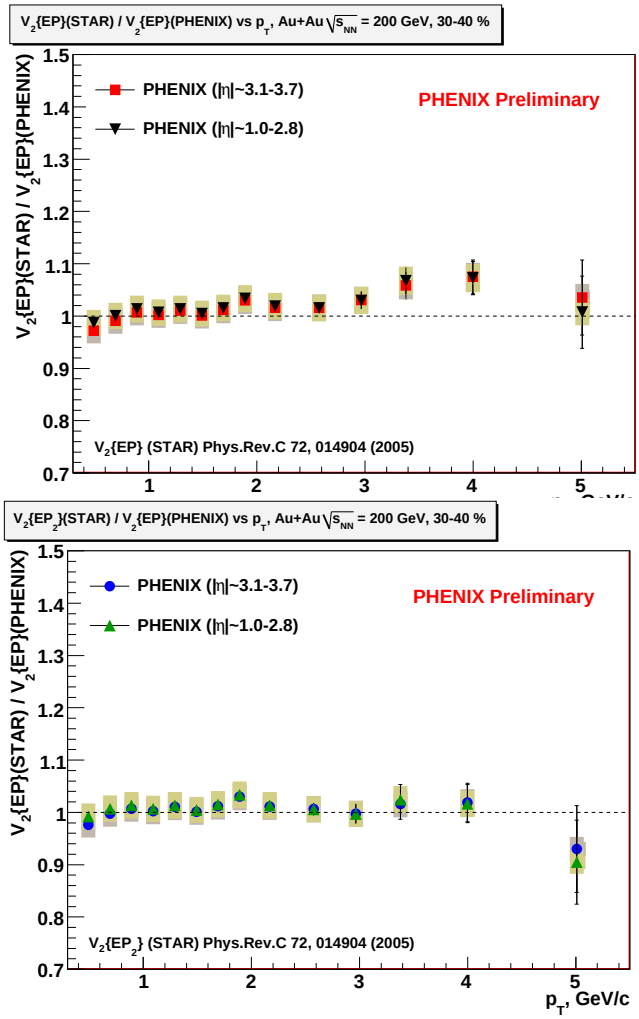

Figure 20: Upper panel: p_T dependence of the ratio of STAR v_2 values obtained by standard event plane method $v_2\{\mathrm{EP}\}$ using central TPC ($|\eta| < 1.0$) to the PHENIX v_2 values obtained by event plane method using MPC/RXN event planes for 30-40% central Au+Au collisions. Lower panel: p_T dependence of the ratio of STAR v_2 values obtained by modified event plane method $v_2\{\mathrm{EP}_2\}$ to the same PHENIX v_2 values. The STAR v_2 data are taken from [2]

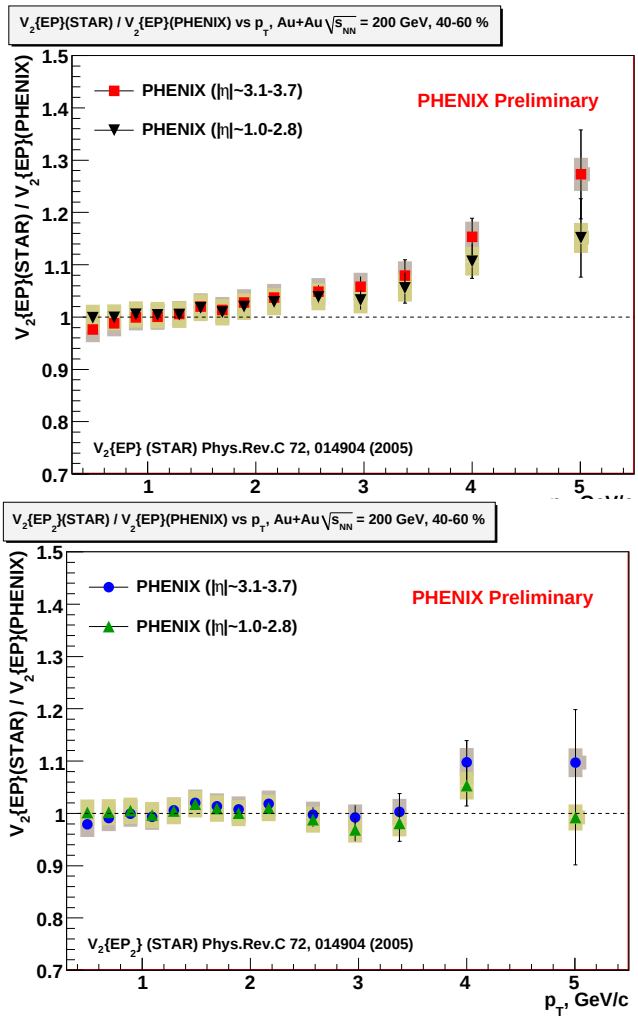

Figure 21: Upper panel: p_T dependence of the ratio of STAR v_2 values obtained by standard event plane method $v_2\{\mathrm{EP}\}$ using central TPC ($|\eta| < 1.0$) to the PHENIX v_2 values obtained by event plane method using MPC/RXN event planes for 40-60% central Au+Au collisions. Lower panel: p_T dependence of the ratio of STAR v_2 values obtained by modified event plane method $v_2\{\mathrm{EP}_2\}$ to the same PHENIX v_2 values. The STAR v_2 data are taken from [2]

4.3 Modified Two-Particle Correlation Method: $v_2\{v_2\text{-pp}\}$

.

The next comparison will be done for STAR v_2 values obtained by Two-particle correlation method with subtraction the correlations measured in p+p collisions $v_2\{v_2\text{-pp}\}$, details of the method can be found in [2, 3]. The published STAR $v_2\{v_2\text{-pp}\}$ data are available for 20-60% mid-central Au+Au collisions only [3].

Figure 22 shows the p_T dependence of the ratio of STAR $v_2\{v_2\text{-pp}\}$ values to the PHENIX v_2 values obtained by event plane method using event plane from MPC ($3.1 < |\eta| < 3.7$) [closed red circles] and RXN detector ($1.0 < |\eta| < 2.8$) [closed blue boxes]. As one can see that for this particular centrality selection the difference between STAR/PHENIX v_2 values is less than 5-6% for the present p_T range although the ratio $v_2\{v_2\text{-pp}\}$(STAR)/$v_2\{\text{EP}\}$(PHENIX) seems to have small p_T dependence for the present centrality selection.

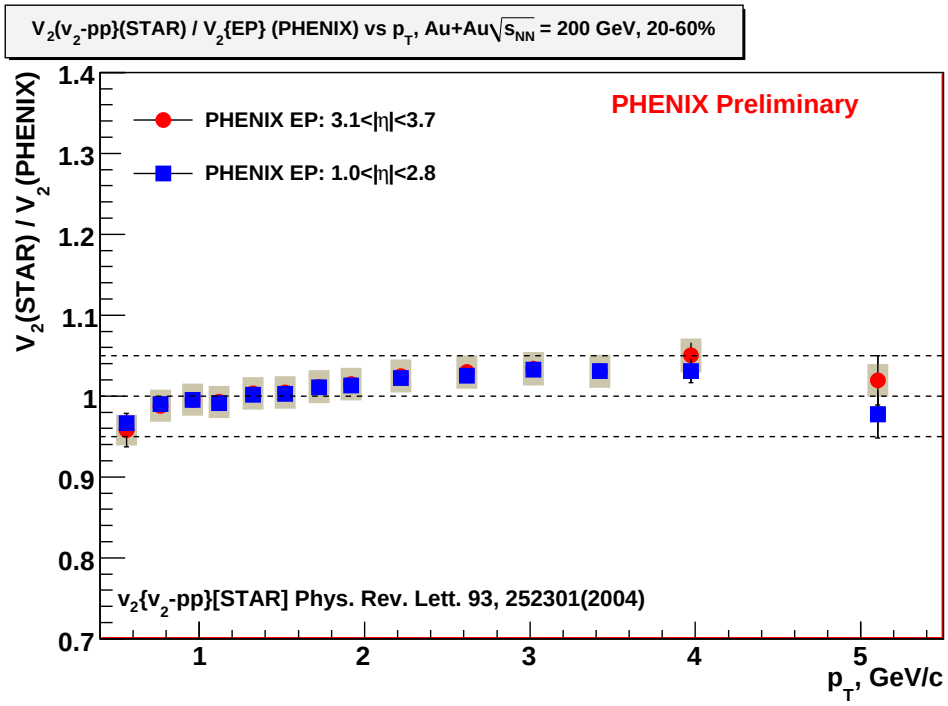

Figure 22: p_T dependence of the ratio of STAR v_2 values obtained by two-particle correlation method with subtraction the correlations measured in p+p collisions $v_2\{v_2\text{-pp}\}$ using central TPC ($|\eta| < 1.0$) to the PHENIX v_2 values obtained by event plane method using event plane from MPC ($3.1 < |\eta| < 3.7$) [closed red circles] and RXN detector ($1.0 < |\eta| < 2.8$) [closed blue boxes]. The comparison was made for v_2 of charged hadrons from 20-60% mid-central Au+Au collisions at $\sqrt{s_{NN}} = 200$-GeV. The STAR v_2 data were taken from [3]

4.4 Two-Particle Cumulant Method: $v_2\{2\}$

The results for published STAR v_2 data obtained by two-particle cumulant method is available also for 20-60% mid-central Au+Au collisions [2, 3]. Figure 23 shows the p_T dependence of the ratio of STAR $v_2\{2\}$ values obtained by two-particle cumulant method to the PHENIX v_2 values obtained by event plane method using event plane from MPC ($3.1 < |\eta| < 3.7$) [closed red triangles] and RXN detector ($1.0 < |\eta| < 2.8$) [open blue boxes]. As one can see that for this particular centrality selection the difference between STAR $v_2\{2\}$ and PHENIX v_2EP values is rather large and has strong p_T dependense. It is very hard to understand why STAR $v_2\{2\}$ and $v_2\{EP\}$ results are so different.

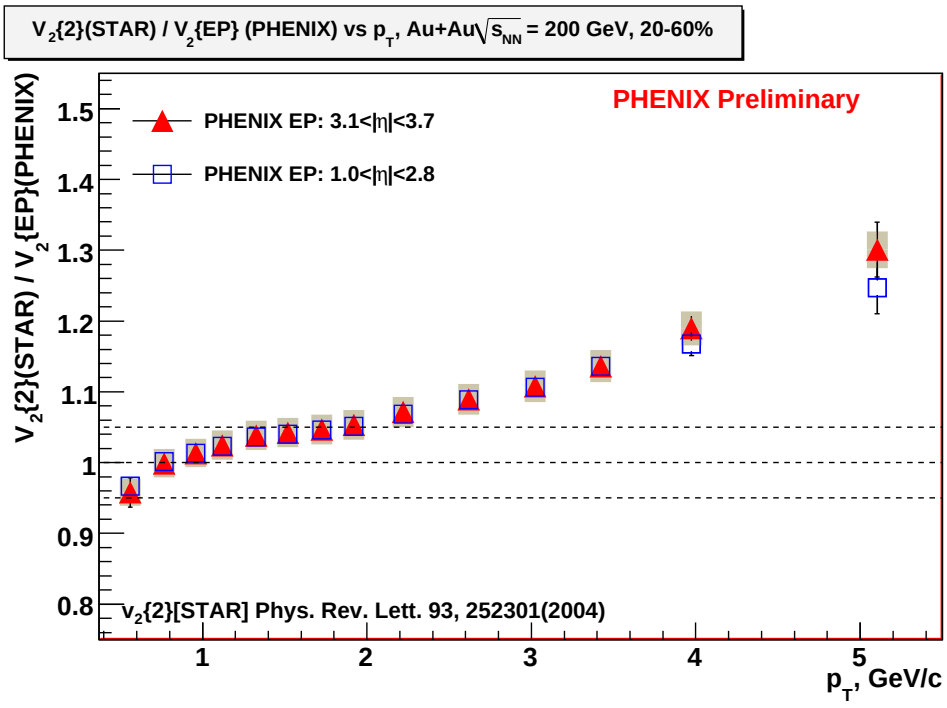

Figure 23: p_T dependence of the ratio of STAR v_2 values obtained by two-particle cumulant method $v_2\{2\}$ using charged tracks from central TPC ($|\eta| < 1.0$) to the PHENIX v_2 values obtained by event plane method using event plane from MPC ($3.1 < |\eta| < 3.7$) [closed red triangles] and RXN detector ($1.0 < |\eta| < 2.8$) [open blue boxes]. The comparison was made for v_2 of charged hadrons from 20-60% mid-central Au+Au collisions at$\sqrt{s_{NN}}$ = 200-GeV. The STAR v_2 data were taken from [3]

4.5 Four-Particle Cumulant Method: $v_2\{4\}$

The results for published STAR v_2 data obtained by 4-particle cumulant method $v_2\{4\}$ are available for 20-60% mid-central Au+Au collisions [2, 3, 4]. Figure 24 shows the p_T dependence of the ratio of STAR $v_2\{2\}$ values obtained by four-particle cumulant method to the PHENIX v_2 values obtained by event plane method using event plane from MPC ($3.1 < |\eta| < 3.7$) [closed red triangles] and RXN detector ($1.0 < |\eta| < 2.8$) [open blue boxes]. PHENIX $v_2\{\mathrm{EP}\}$ event plane results are found to be smaller than STAR $v_2\{4\}$ by 10-15% for this centrality selection.

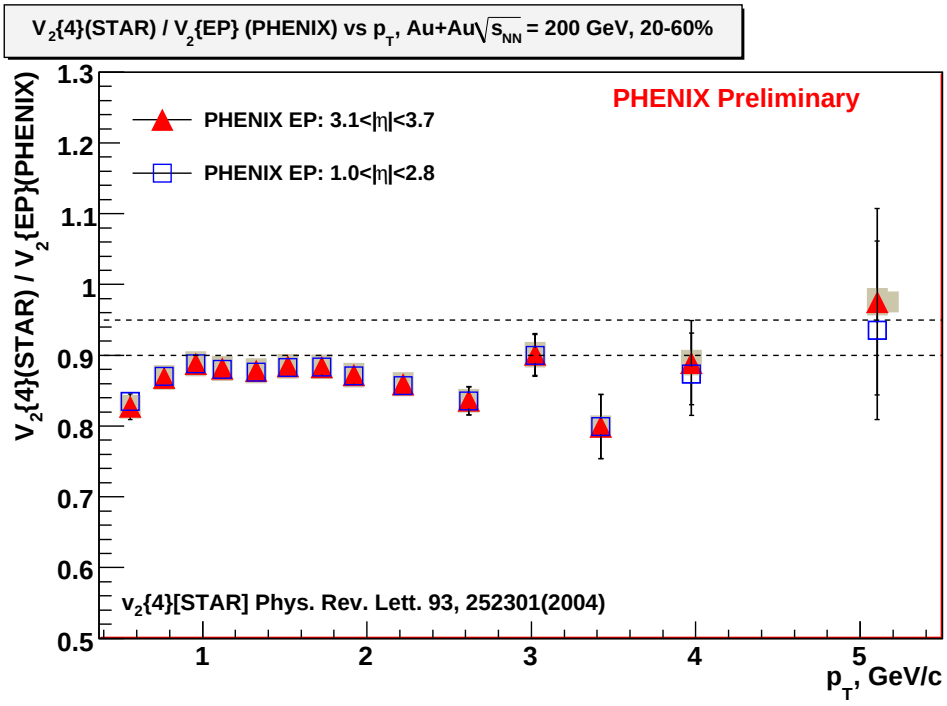

Figure 24: p_T dependence of the ratio of STAR v_2 values obtained by four-particle cumulant method $v_2\{4\}$ using charged tracks from central TPC ($|\eta| < 1.0$) to the PHENIX v_2 values obtained by event plane method using event plane from MPC ($3.1 < |\eta| < 3.7$) [closed red triangles] and RXN detector ($1.0 < |\eta| < 2.8$) [open blue boxes]. The comparison was made for v_2 of charged hadrons from 20-60% mid-central Au+Au collisions at$\sqrt{s_{NN}}$ = 200-GeV. The STAR v_2 data were taken from [3]

4.6 Lee-Yang Zero method: v_2{LYZ}

The results for published STAR v_2 data obtained by Lee-Yang Zero method: v_2{LYZ} are available both for 10-40% central Au+Au collisions only [4]. Figure 25 shows the p_T dependence of the ratio of STAR v_2{LYZ} values obtained by Lee-Yang Zero method to the PHENIX v_2 values obtained by event plane method using event plane from MPC ($3.1 < |\eta| < 3.7$) [closed red triangles] and RXN detector ($1.0 < |\eta| < 2.8$) [open blue boxes]. PHENIX v_2{EP} event plane results are found to be smaller than STAR v_2{LYZ} by 10-12% for this centrality selection and the difference looks like does not depends on p_T.

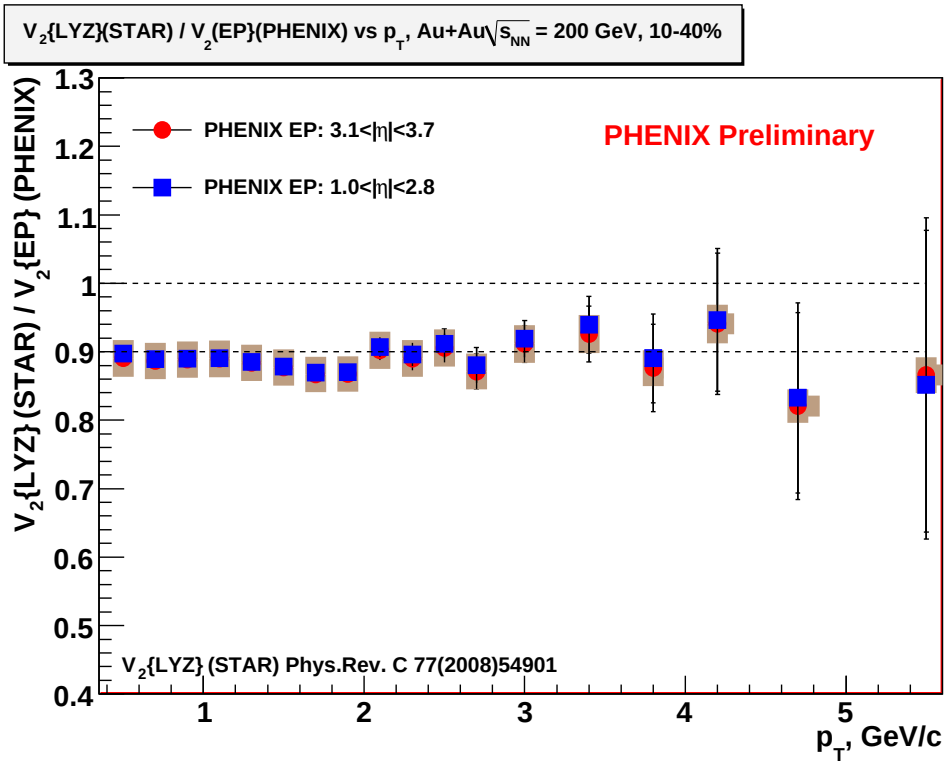

Figure 25: p_T dependence of the ratio of STAR v_2 values obtained by Lee-Yang Zero method: v_2{LYZ} using charged tracks from central TPC ($|\eta| < 1.0$) to the PHENIX v_2 values obtained by event plane method using event plane from MPC ($3.1 < |\eta| < 3.7$) [closed red triangles] and RXN detector ($1.0 < |\eta| < 2.8$) [open blue boxes]. The comparison was made for v_2 of charged hadrons from 10-40% central Au+Au collisions at$\sqrt{s_{NN}} = 200$-GeV. The STAR v_2 data were taken from [4]

5 Detailed p_T/centrality comparison for v_2 between PHENIX/STAR

The published STAR v_2 data for charged hadrons from Au+Au collisions at 200 GeV which allow to perform the detailed centrality/p_T comparison with PHENIX data are available only for the standard event plane method $v_2\{\mathrm{EP}\}$ and modified event plane $v_2\{EP_2\}$ methods using STAR TPC [2].

The upper panels of Figures 26- 31 show the p_T dependence of the ratio of STAR v_2 values obtained by standard event plane method $v_2\{\mathrm{EP}\}$ to the PHENIX v_2 values obtained by event plane method using MPC/RXN event planes for three bins in collision centrality: 0-5%, 5-10% , 10-20%, 20-30%, 30-40% and 40-60%. The lower panels of Figures 19- 21 show the same ratios but in this case the STAR v_2 data were obtained using modified event plane method $v_2\{\mathrm{EP}_2\}$. The trends are the same as already was observed for mid-central collisions: the difference between STAR/PHENIX v_2 at high p_T is getting much smaller for STAR modified event plane $v_2\{\mathrm{EP}_2\}$ data. However from such detailed comparison one see another trend that in central 0-20% collisions the STAR $v_2\{\mathrm{EP}_2\}$ and $v_2\{\mathrm{EP}\}$ data looks like are well above PHENIX v_2 at low p_T. As v_2 is growing very fast with centrality in very central collisions - small difference in centrality definition between STAR and PHENIX may lead to such constant differences in v_2 at low p_T.

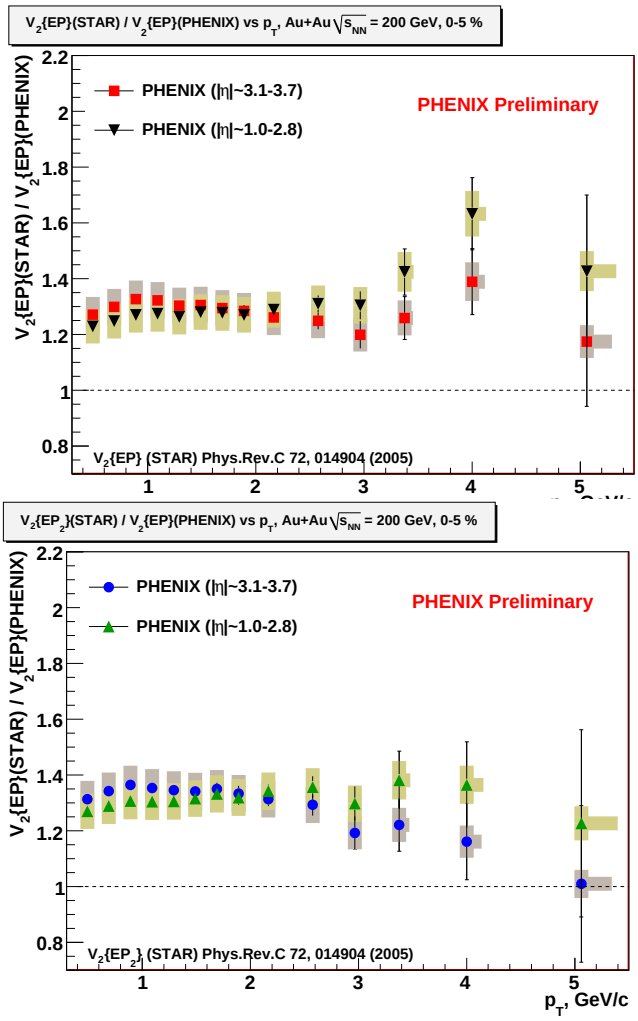

Figure 26: Upper panel: p_T dependence of the ratio of STAR v_2 values obtained by standard event plane method $v_2\{\mathrm{EP}\}$ using central TPC ($|\eta| < 1.0$) to the PHENIX v_2 values obtained by event plane method using MPC/RXN event planes for 0-5% central Au+Au collisions. Lower panel: p_T dependence of the ratio of STAR v_2 values obtained by modified event plane method $v_2\{\mathrm{EP}_2\}$ to the same PHENIX v_2 values. The STAR v_2 data are taken from [2]

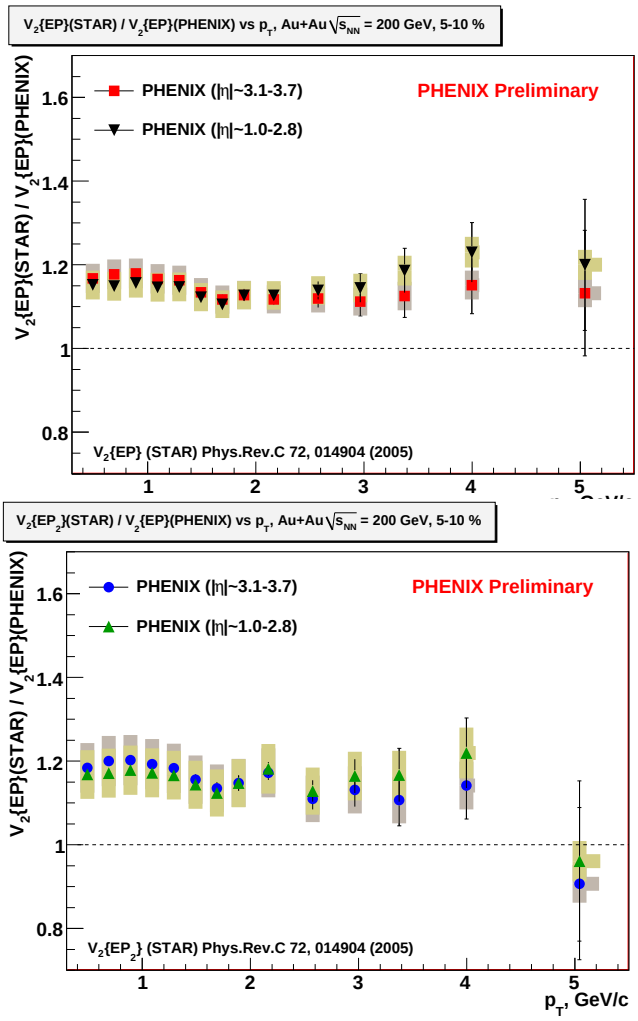

Figure 27: Upper panel: p_T dependence of the ratio of STAR v_2 values obtained by standard event plane method $v_2\{\mathrm{EP}\}$ using central TPC ($|\eta| < 1.0$) to the PHENIX v_2 values obtained by event plane method using MPC/RXN event planes for 5-10% central Au+Au collisions. Lower panel: p_T dependence of the ratio of STAR v_2 values obtained by modified event plane method $v_2\{\mathrm{EP}_2\}$ to the same PHENIX v_2 values. The STAR v_2 data are taken from [2]

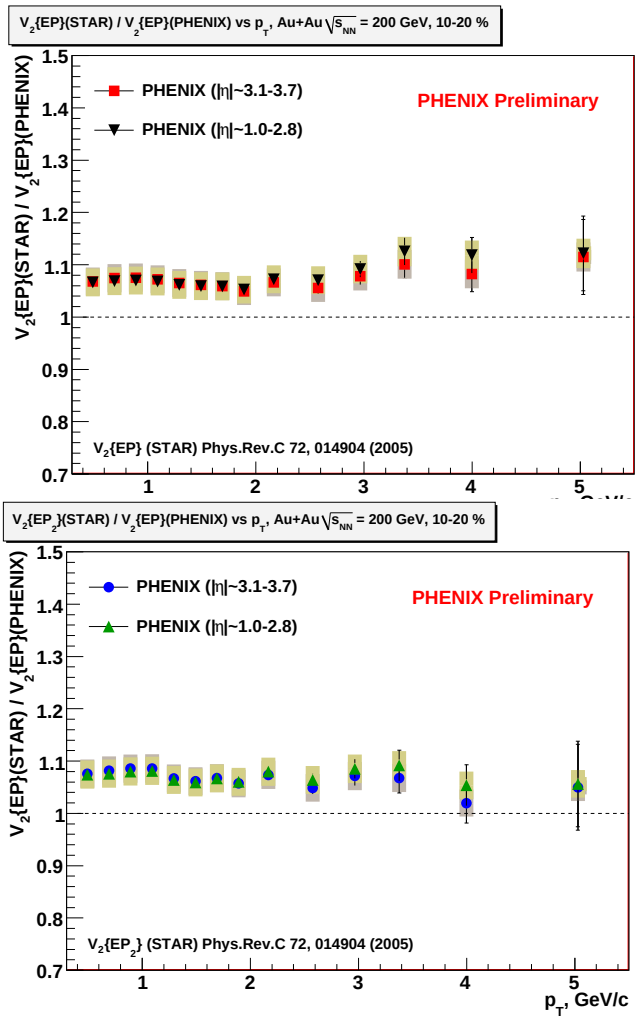

Figure 28: Upper panel: p_T dependence of the ratio of STAR v_2 values obtained by standard event plane method $v_2\{\mathrm{EP}\}$ using central TPC ($|\eta| < 1.0$) to the PHENIX v_2 values obtained by event plane method using MPC/RXN event planes for 10-20% central Au+Au collisions. Lower panel: p_T dependence of the ratio of STAR v_2 values obtained by modified event plane method $v_2\{\mathrm{EP}_2\}$ to the same PHENIX v_2 values. The STAR v_2 data are taken from [2]

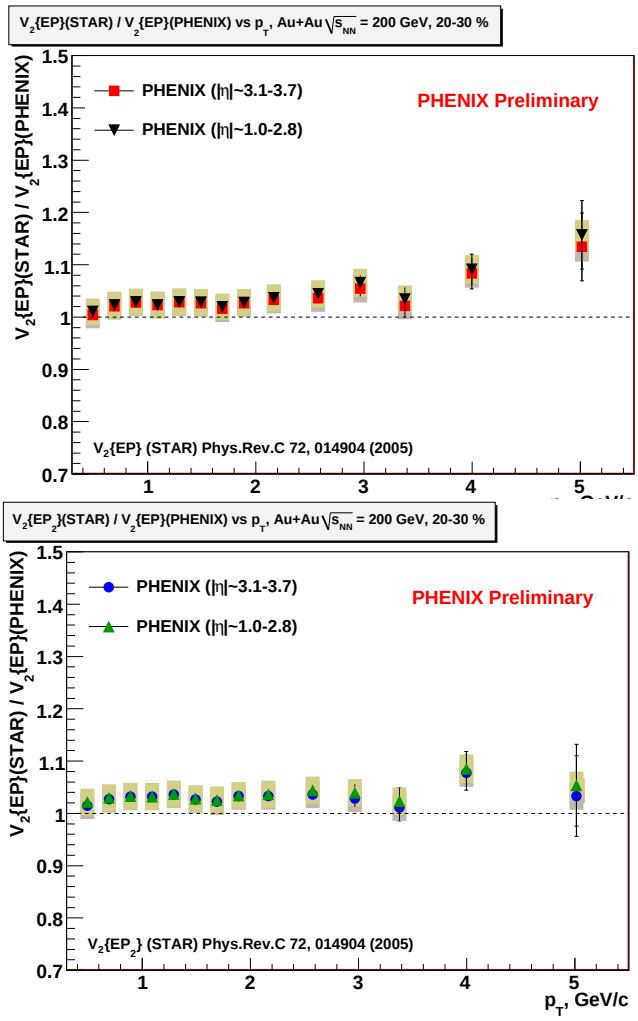

Figure 29: Upper panel: p_T dependence of the ratio of STAR v_2 values obtained by standard event plane method $v_2\{\mathrm{EP}\}$ using central TPC ($|\eta| < 1.0$) to the PHENIX v_2 values obtained by event plane method using MPC/RXN event planes for 20-30% central Au+Au collisions. Lower panel: p_T dependence of the ratio of STAR v_2 values obtained by modified event plane method $v_2\{\mathrm{EP}_2\}$ to the same PHENIX v_2 values. The STAR v_2 data are taken from [2]

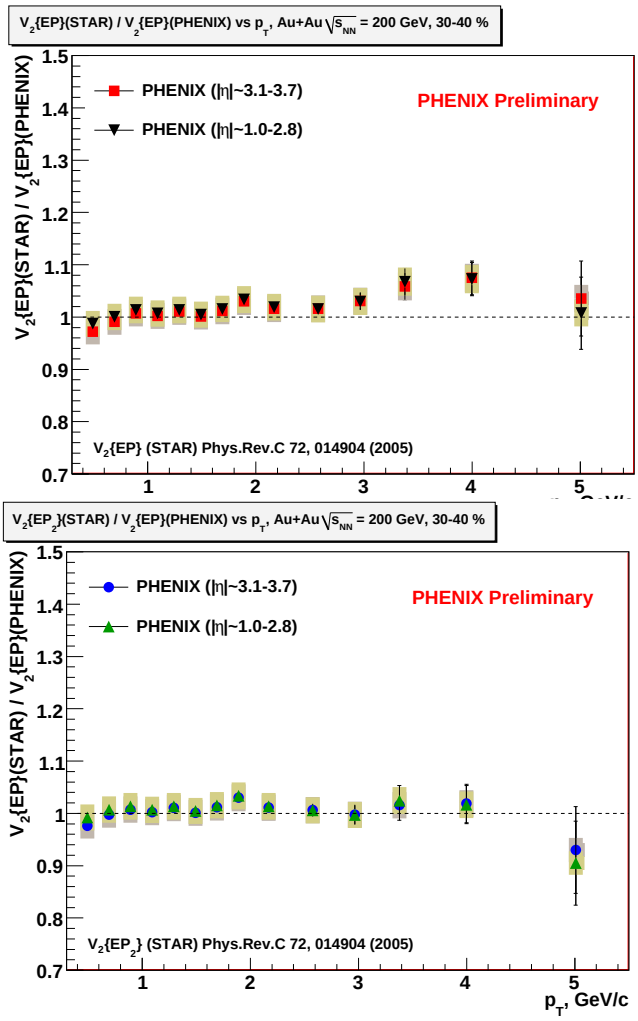

Figure 30: Upper panel: p_T dependence of the ratio of STAR v_2 values obtained by standard event plane method $v_2\{\mathrm{EP}\}$ using central TPC ($|\eta| < 1.0$) to the PHENIX v_2 values obtained by event plane method using MPC/RXN event planes for 30-40% central Au+Au collisions. Lower panel: p_T dependence of the ratio of STAR v_2 values obtained by modified event plane method $v_2\{\mathrm{EP}_2\}$ to the same PHENIX v_2 values. The STAR v_2 data are taken from [2]

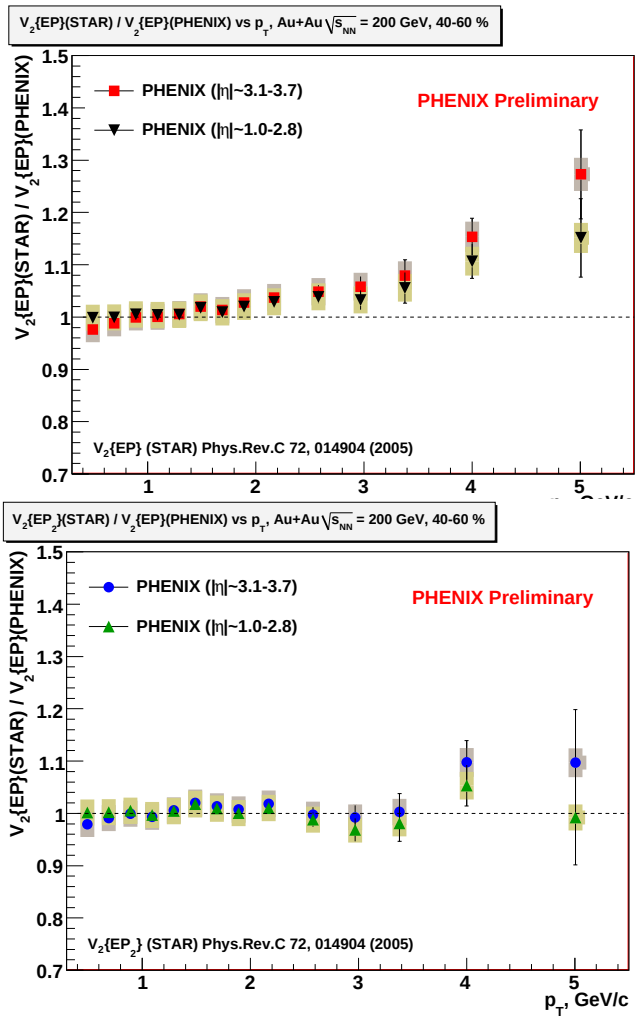

Figure 31: Upper panel: p_T dependence of the ratio of STAR v_2 values obtained by standard event plane method $v_2\{\mathrm{EP}\}$ using central TPC ($|\eta| < 1.0$) to the PHENIX v_2 values obtained by event plane method using MPC/RXN event planes for 40-60% central Au+Au collisions. Lower panel: p_T dependence of the ratio of STAR v_2 values obtained by modified event plane method $v_2\{\mathrm{EP}_2\}$ to the same PHENIX v_2 values. The STAR v_2 data are taken from [2]

6 Comparison with PHOBOS $v_2(p_T$,centrality) results

As it was mentioned before the only published data for PHOBOS $v_2(p_T)$ for charged hadrons emitted in Au+Au collisions at 200 GeV are available for a very broad centrality selection 0-50% [5]. However the "preliminary" PHOBOS v_2 data for $v_2(p_T)$ for 0-20, 20-40 and 35-50% central Au+Au collisions at 200 GeV are available from Rachid Nouicer QM2006 proceedings [12]. PHOBOS $v_2(p_T)$ were performed for charged hadrons with $(0 < \eta < 1.5)$ with respect to the second order event plane measured at $(2.05 < \eta < 3.2)$ [5][**???**], which very close the η coverage of RXN/MPC. The v_2 ratios $v_2\{\mathrm{EP}\}(\mathrm{PHOBOS})/v_2\{\mathrm{EP}\}(\mathrm{PHENIX})$ are plotted on figures 32- 33 as a function fo p_T for several bins in collision centrality as indicated. According to this ratio plots the difference between PHENIX/PHOBOS v_2 results are $\leq 5\%$ and does not show clear p_T dependence.

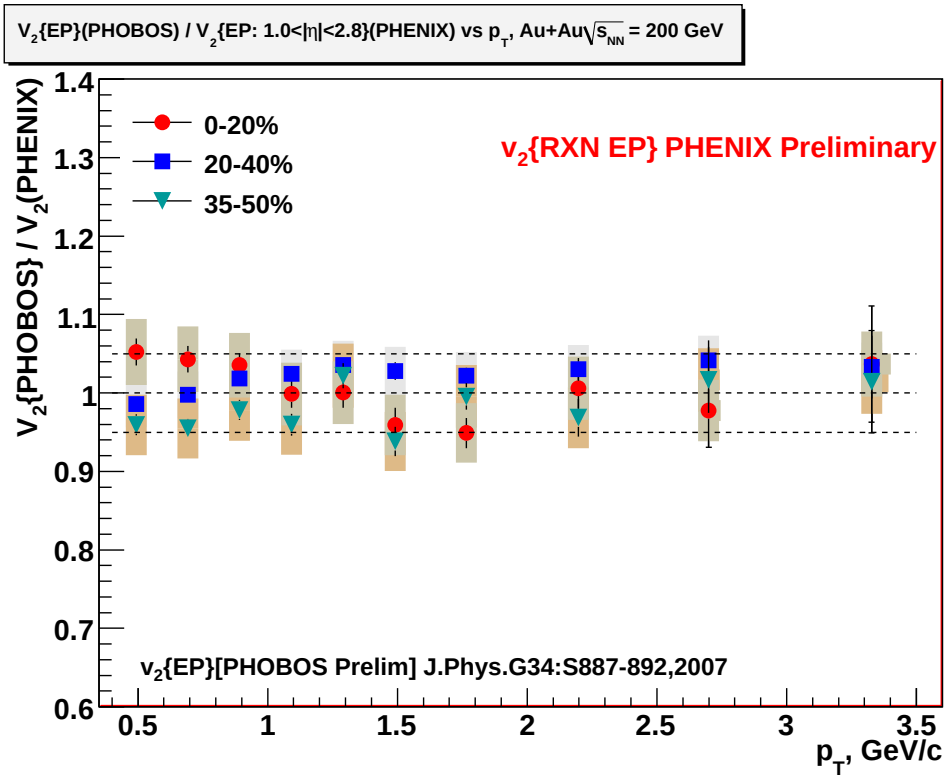

Figure 32: p_T dependence of the ratio of PHOBOS v_2 values obtained by standard event plane method $v_2\{\mathrm{EP}\}$ $(2.05 < |\eta| < 3.2)$ to the PHENIX v_2 values obtained by event plane method using event plane from RXN detector $(1.0 < |\eta| < 2.8)$ for several bins in collision centrality as indicated. The comparison was made for v_2 of charged hadrons from Au+Au collisions at $\sqrt{s_{NN}} = 200$-GeV. The PHOBOS v_2 data were taken from [12].

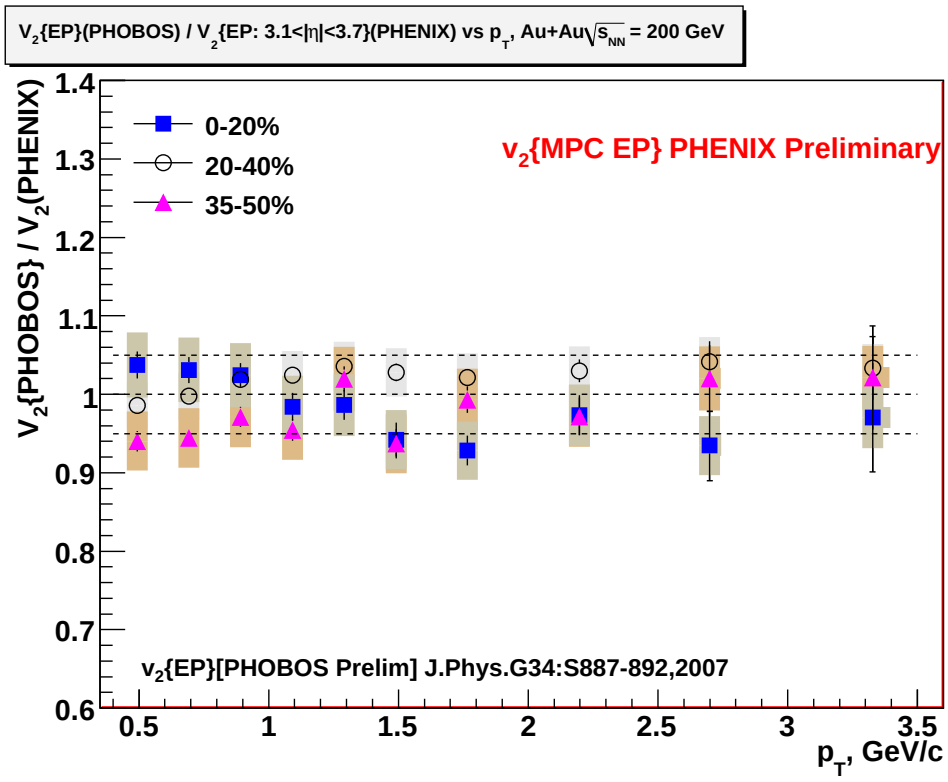

Figure 33: p_T dependence of the ratio of PHOBOS v_2 values obtained by standard event plane method $v_2\{\mathrm{EP}\}$ ($2.05 < |\eta| < 3.2$) to the PHENIX v_2 values obtained by event plane method using event plane from MPC detector ($3.1 < |\eta| < 3.7$) for several bins in collision centrality as indicated. The comparison was made for v_2 of charged hadrons from Au+Au collisions at$\sqrt{s_{NN}} = 200$-GeV. The PHOBOS v_2 data were taken from [12].

7 Deta tables with $v_2(p_T, centrality\ )$ results

Table 1: v_2 of charged hadrons as a function of p_T. The measurements are performed with respect to the combined **RXN and MPC event planes for 0-5% central collisions**.

$p_T(GeV/c)$	$v_2(RXN)$	$\sigma_{stat}(v_2)$	$v_2(MPC)$	$\sigma_{stat}(v_2)$
0.425	0.0123	0.000065	0.0119	0.000113
0.475	0.0140	0.000068	0.0133	0.000119
0.525	0.0158	0.000071	0.0154	0.000125
0.574	0.0175	0.000075	0.0168	0.000132
0.624	0.0194	0.000080	0.0184	0.000140
0.674	0.0210	0.000085	0.0201	0.000149
0.724	0.0224	0.000090	0.0217	0.000158
0.775	0.0241	0.000096	0.0232	0.000168
0.824	0.0255	0.000101	0.0244	0.000178
0.875	0.0272	0.000108	0.0259	0.000190
0.925	0.0284	0.000114	0.0273	0.000201
0.974	0.0299	0.000121	0.0286	0.000213
1.048	0.0318	0.000094	0.0306	0.000165
1.148	0.0345	0.000105	0.0331	0.000185
1.248	0.0371	0.000118	0.0358	0.000208
1.348	0.0397	0.000133	0.0386	0.000234
1.448	0.0419	0.000150	0.0408	0.000264
1.548	0.0443	0.000171	0.0438	0.000300
1.648	0.0468	0.000194	0.0457	0.000340
1.748	0.0482	0.000219	0.0476	0.000385
1.848	0.0502	0.000248	0.0495	0.000436
1.948	0.0521	0.000281	0.0517	0.000494
2.091	0.0538	0.000239	0.0547	0.000421
2.292	0.0556	0.000309	0.0571	0.000543
2.492	0.0577	0.000395	0.0598	0.000695
2.692	0.0584	0.000503	0.0615	0.000885
2.892	0.0575	0.000637	0.0606	0.001121
3.093	0.0560	0.000802	0.0636	0.001410
3.334	0.0578	0.001036	0.0632	0.001823
3.675	0.0520	0.001332	0.0623	0.002343
4.118	0.0458	0.001858	0.0560	0.003270
4.584	0.0452	0.003093	0.0523	0.005441
5.031	0.0457	0.003829	0.0475	0.006732
5.445	0.0397	0.006332	0.0654	0.011119
5.972	0.0482	0.005103	0.0505	0.008978
6.687	0.0511	0.007997	0.0723	0.014038

Table 2: v_2 of charged hadrons as a function of p_T. The measurements are performed with respect to the combined **RXN and MPC event planes for 5-10% central collisions**.

$p_T(GeV/c)$	$v_2(RXN)$	$\sigma_{stat}(v_2)$	$v_2(MPC)$	$\sigma_{stat}(v_2)$
0.425	0.0206	0.000056	0.0204	0.000086
0.475	0.0234	0.000058	0.0232	0.000090
0.525	0.0263	0.000061	0.0258	0.000095
0.575	0.0290	0.000065	0.0286	0.000100
0.624	0.0318	0.000068	0.0310	0.000106
0.675	0.0344	0.000073	0.0336	0.000112
0.724	0.0371	0.000077	0.0361	0.000119
0.775	0.0396	0.000082	0.0386	0.000127
0.824	0.0419	0.000087	0.0411	0.000134
0.875	0.0441	0.000092	0.0432	0.000143
0.925	0.0467	0.000098	0.0459	0.000151
0.975	0.0487	0.000104	0.0476	0.000160
1.048	0.0519	0.000080	0.0511	0.000124
1.148	0.0563	0.000089	0.0552	0.000139
1.248	0.0603	0.000101	0.0595	0.000156
1.348	0.0645	0.000113	0.0635	0.000175
1.448	0.0688	0.000128	0.0682	0.000198
1.548	0.0729	0.000145	0.0719	0.000225
1.648	0.0761	0.000164	0.0750	0.000254
1.748	0.0799	0.000186	0.0793	0.000287
1.848	0.0831	0.000210	0.0827	0.000325
1.948	0.0857	0.000237	0.0858	0.000368
2.092	0.0897	0.000202	0.0900	0.000313
2.292	0.0934	0.000259	0.0948	0.000401
2.492	0.0969	0.000331	0.0982	0.000512
2.692	0.0990	0.000420	0.1008	0.000650
2.892	0.0988	0.000530	0.1018	0.000820
3.093	0.1013	0.000776	0.1045	0.001202
3.334	0.1014	0.000861	0.1076	0.001333
3.675	0.0983	0.001102	0.1030	0.001707
4.117	0.0913	0.001537	0.0981	0.002378
4.583	0.0858	0.002549	0.0897	0.003940
5.030	0.0858	0.003177	0.0895	0.004918
5.444	0.0826	0.005294	0.0873	0.008222
5.969	0.0696	0.004312	0.0802	0.006675
6.686	0.0722	0.006775	0.0662	0.010547

Table 3: v_2 of charged hadrons as a function of p_T. The measurements are performed with respect to the combined **RXN and MPC event planes for 10-20% central collisions**.

$p_T(GeV/c)$	$v_2(RXN)$	$\sigma_{stat}(v_2)$	$v_2(MPC)$	$\sigma_{stat}(v_2)$
0.425	0.0327	0.000038	0.0326	0.000055
0.475	0.0368	0.000040	0.0368	0.000058
0.525	0.0410	0.000042	0.0410	0.000061
0.575	0.0452	0.000044	0.0450	0.000064
0.625	0.0492	0.000047	0.0490	0.000068
0.675	0.0530	0.000050	0.0528	0.000072
0.724	0.0569	0.000053	0.0565	0.000076
0.775	0.0605	0.000056	0.0602	0.000081
0.824	0.0641	0.000059	0.0636	0.000085
0.875	0.0674	0.000063	0.0669	0.000091
0.925	0.0707	0.000067	0.0705	0.000096
0.975	0.0740	0.000071	0.0737	0.000102
1.048	0.0787	0.000054	0.0783	0.000078
1.148	0.0849	0.000061	0.0846	0.000088
1.248	0.0911	0.000068	0.0908	0.000099
1.348	0.0972	0.000077	0.0968	0.000111
1.448	0.1029	0.000087	0.1027	0.000125
1.548	0.1088	0.000098	0.1085	0.000142
1.648	0.1137	0.000111	0.1134	0.000161
1.748	0.1188	0.000126	0.1190	0.000181
1.848	0.1232	0.000142	0.1235	0.000205
1.948	0.1276	0.000160	0.1280	0.000231
2.092	0.1325	0.000136	0.1333	0.000196
2.292	0.1386	0.000174	0.1394	0.000251
2.492	0.1427	0.000221	0.1443	0.000319
2.692	0.1456	0.000279	0.1482	0.000403
2.892	0.1471	0.000351	0.1488	0.000507
3.093	0.1493	0.000515	0.1520	0.000745
3.334	0.1484	0.000570	0.1510	0.000824
3.675	0.1446	0.000726	0.1487	0.001049
4.117	0.1373	0.001005	0.1422	0.001453
4.582	0.1280	0.001673	0.1309	0.002414
5.028	0.1199	0.002087	0.1228	0.003015
5.444	0.1154	0.003511	0.1091	0.005062
5.965	0.1088	0.002863	0.1020	0.004127
6.685	0.1070	0.004605	0.1120	0.006661

Table 4: v_2 of charged hadrons as a function of p_T. The measurements are performed with respect to the combined **RXN and MPC event planes for 20-30% central collisions**.

$p_T(GeV/c)$	$v_2(RXN)$	$\sigma_{stat}(v_2)$	$v_2(MPC)$	$\sigma_{stat}(v_2)$
0.425	0.0457	0.000043	0.0460	0.000061
0.475	0.0513	0.000045	0.0517	0.000064
0.525	0.0569	0.000048	0.0572	0.000067
0.575	0.0624	0.000050	0.0628	0.000070
0.625	0.0677	0.000053	0.0680	0.000074
0.675	0.0729	0.000056	0.0731	0.000079
0.724	0.0778	0.000059	0.0780	0.000084
0.775	0.0827	0.000063	0.0828	0.000089
0.824	0.0872	0.000067	0.0873	0.000094
0.875	0.0918	0.000071	0.0918	0.000100
0.925	0.0962	0.000075	0.0962	0.000105
0.975	0.1004	0.000080	0.1006	0.000112
1.048	0.1066	0.000061	0.1066	0.000086
1.148	0.1148	0.000069	0.1149	0.000097
1.248	0.1228	0.000077	0.1229	0.000109
1.348	0.1303	0.000087	0.1305	0.000122
1.448	0.1377	0.000098	0.1379	0.000138
1.548	0.1447	0.000111	0.1450	0.000156
1.648	0.1511	0.000125	0.1516	0.000176
1.748	0.1573	0.000141	0.1576	0.000199
1.848	0.1629	0.000159	0.1632	0.000224
1.948	0.1678	0.000179	0.1680	0.000253
2.092	0.1736	0.000152	0.1740	0.000214
2.292	0.1802	0.000193	0.1812	0.000273
2.492	0.1846	0.000244	0.1860	0.000345
2.692	0.1872	0.000307	0.1890	0.000435
2.893	0.1882	0.000385	0.1892	0.000544
3.093	0.1873	0.000478	0.1894	0.000676
3.335	0.1883	0.000625	0.1918	0.000883
3.675	0.1830	0.000790	0.1841	0.001117
4.116	0.1737	0.001089	0.1753	0.001538
4.582	0.1627	0.001803	0.1691	0.002542
5.027	0.1553	0.002249	0.1538	0.003178
5.443	0.1399	0.003811	0.1375	0.005380
5.961	0.1416	0.003131	0.1350	0.004417
6.683	0.1380	0.005034	0.1339	0.007140

Table 5: v_2 of charged hadrons as a function of p_T. The measurements are performed with respect to the combined **RXN and MPC event planes for 30-40% central collisions**.

$p_T(GeV/c)$	$v_2(RXN)$	$\sigma_{stat}(v_2)$	$v_2(MPC)$	$\sigma_{stat}(v_2)$
0.425	0.0543	0.000055	0.0554	0.000079
0.475	0.0610	0.000057	0.0621	0.000083
0.525	0.0678	0.000060	0.0688	0.000087
0.575	0.0744	0.000063	0.0752	0.000091
0.625	0.0806	0.000067	0.0815	0.000096
0.675	0.0868	0.000071	0.0875	0.000102
0.724	0.0925	0.000075	0.0932	0.000108
0.775	0.0978	0.000080	0.0989	0.000115
0.824	0.1032	0.000085	0.1041	0.000122
0.875	0.1086	0.000090	0.1093	0.000129
0.925	0.1138	0.000095	0.1144	0.000137
0.975	0.1188	0.000101	0.1195	0.000145
1.048	0.1258	0.000078	0.1265	0.000112
1.148	0.1352	0.000087	0.1357	0.000126
1.248	0.1440	0.000098	0.1446	0.000142
1.348	0.1526	0.000110	0.1531	0.000159
1.448	0.1609	0.000124	0.1614	0.000180
1.548	0.1681	0.000141	0.1687	0.000204
1.648	0.1751	0.000159	0.1758	0.000230
1.748	0.1816	0.000180	0.1823	0.000260
1.848	0.1870	0.000203	0.1877	0.000293
1.948	0.1924	0.000229	0.1932	0.000330
2.092	0.1984	0.000193	0.1989	0.000279
2.292	0.2049	0.000245	0.2055	0.000354
2.492	0.2088	0.000309	0.2087	0.000447
2.693	0.2112	0.000387	0.2111	0.000561
2.893	0.2111	0.000483	0.2111	0.000699
3.093	0.2112	0.000714	0.2115	0.001033
3.335	0.2089	0.000783	0.2109	0.001132
3.676	0.2033	0.000983	0.2035	0.001421
4.117	0.1946	0.001345	0.1933	0.001941
4.582	0.1841	0.002219	0.1825	0.003198
5.026	0.1750	0.002762	0.1662	0.003985
5.443	0.1604	0.004687	0.1525	0.006733
5.958	0.1585	0.003857	0.1528	0.005553
6.682	0.1569	0.006338	0.1309	0.009161

Table 6: v_2 of charged hadrons as a function of p_T. The measurements are performed with respect to the combined **RXN and MPC event planes for 40-50% central collisions**.

$p_T(GeV/c)$	$v_2(RXN)$	$\sigma_{stat}(v_2)$	$v_2(MPC)$	$\sigma_{stat}(v_2)$
0.425	0.0587	0.000078	0.0605	0.000118
0.475	0.0660	0.000081	0.0679	0.000124
0.525	0.0735	0.000085	0.0749	0.000130
0.575	0.0803	0.000090	0.0819	0.000137
0.625	0.0873	0.000095	0.0887	0.000145
0.675	0.0939	0.000100	0.0953	0.000153
0.724	0.1003	0.000107	0.1015	0.000163
0.775	0.1062	0.000113	0.1073	0.000173
0.824	0.1120	0.000120	0.1133	0.000183
0.875	0.1178	0.000128	0.1190	0.000195
0.924	0.1234	0.000136	0.1243	0.000207
0.974	0.1287	0.000144	0.1296	0.000220
1.048	0.1361	0.000111	0.1372	0.000170
1.148	0.1461	0.000125	0.1467	0.000191
1.248	0.1554	0.000141	0.1555	0.000216
1.348	0.1642	0.000159	0.1649	0.000244
1.448	0.1725	0.000180	0.1730	0.000275
1.548	0.1801	0.000204	0.1802	0.000313
1.648	0.1866	0.000231	0.1872	0.000353
1.748	0.1928	0.000260	0.1929	0.000399
1.848	0.1985	0.000294	0.1985	0.000450
1.948	0.2030	0.000331	0.2027	0.000508
2.092	0.2083	0.000279	0.2081	0.000429
2.292	0.2138	0.000354	0.2132	0.000543
2.492	0.2169	0.000445	0.2173	0.000683
2.693	0.2178	0.000557	0.2169	0.000854
2.893	0.2182	0.000691	0.2150	0.001061
3.093	0.2152	0.000852	0.2129	0.001307
3.335	0.2142	0.001115	0.2123	0.001711
3.676	0.2077	0.001391	0.2078	0.002134
4.117	0.2023	0.001885	0.1942	0.002893
4.582	0.1880	0.003091	0.1840	0.004737
5.026	0.1862	0.003855	0.1681	0.005907
5.442	0.1734	0.006507	0.1663	0.010002
5.957	0.1775	0.005373	0.1599	0.008244
6.680	0.1883	0.008784	0.1638	0.013484

Table 7: v_2 of charged hadrons as a function of p_T. The measurements are performed with respect to the combined **RXN and MPC event planes for 10-40% central collisions**.

$p_T(GeV/c)$	$v_2(RXN)$	$\sigma_{stat}(v_2)$	$v_2(MPC)$	$\sigma_{stat}(v_2)$
0.425	0.0418	0.000025	0.0422	0.000036
0.475	0.0470	0.000027	0.0474	0.000038
0.525	0.0523	0.000028	0.0526	0.000040
0.575	0.0574	0.000029	0.0577	0.000042
0.625	0.0624	0.000031	0.0626	0.000044
0.675	0.0671	0.000033	0.0673	0.000047
0.724	0.0718	0.000035	0.0719	0.000050
0.775	0.0762	0.000037	0.0764	0.000053
0.824	0.0805	0.000039	0.0806	0.000056
0.875	0.0847	0.000042	0.0847	0.000060
0.925	0.0888	0.000044	0.0889	0.000063
0.975	0.0927	0.000047	0.0929	0.000067
1.048	0.0985	0.000036	0.0985	0.000052
1.148	0.1060	0.000040	0.1061	0.000058
1.248	0.1133	0.000045	0.1135	0.000065
1.348	0.1204	0.000051	0.1205	0.000073
1.448	0.1273	0.000057	0.1275	0.000082
1.548	0.1338	0.000065	0.1340	0.000093
1.648	0.1397	0.000074	0.1400	0.000106
1.748	0.1455	0.000083	0.1460	0.000119
1.848	0.1506	0.000094	0.1510	0.000135
1.948	0.1553	0.000106	0.1559	0.000152
2.092	0.1609	0.000090	0.1617	0.000129
2.292	0.1674	0.000114	0.1684	0.000164
2.492	0.1717	0.000145	0.1730	0.000208
2.692	0.1745	0.000182	0.1764	0.000262
2.893	0.1757	0.000229	0.1769	0.000328
3.093	0.1772	0.000336	0.1793	0.000483
3.335	0.1758	0.000371	0.1788	0.000532
3.675	0.1714	0.000470	0.1737	0.000674
4.117	0.1633	0.000648	0.1658	0.000929
4.582	0.1533	0.001074	0.1565	0.001537
5.027	0.1452	0.001339	0.1440	0.001919
5.443	0.1345	0.002262	0.1292	0.003236
5.962	0.1316	0.001854	0.1253	0.002651
6.683	0.1290	0.002996	0.1239	0.004304

Table 8: v_2 of charged hadrons as a function of p_T. The measurements are performed with respect to the combined **RXN and MPC event planes for 20-60% central collisions**.

$p_T(GeV/c)$	$v_2(RXN)$	$\sigma_{stat}(v_2)$	$v_2(MPC)$	$\sigma_{stat}(v_2)$
0.425	0.0514	0.000030	0.0520	0.000044
0.475	0.0577	0.000032	0.0584	0.000046
0.525	0.0642	0.000033	0.0646	0.000048
0.575	0.0704	0.000035	0.0708	0.000051
0.625	0.0764	0.000037	0.0767	0.000054
0.675	0.0822	0.000039	0.0823	0.000057
0.724	0.0877	0.000042	0.0878	0.000061
0.775	0.0930	0.000044	0.0931	0.000064
0.824	0.0981	0.000047	0.0982	0.000068
0.875	0.1032	0.000050	0.1032	0.000072
0.925	0.1082	0.000053	0.1080	0.000077
0.974	0.1129	0.000056	0.1128	0.000082
1.048	0.1197	0.000043	0.1195	0.000063
1.148	0.1287	0.000049	0.1284	0.000071
1.248	0.1373	0.000055	0.1369	0.000080
1.348	0.1454	0.000062	0.1451	0.000090
1.448	0.1533	0.000069	0.1530	0.000101
1.548	0.1605	0.000079	0.1602	0.000115
1.648	0.1671	0.000089	0.1670	0.000130
1.748	0.1734	0.000100	0.1731	0.000146
1.848	0.1789	0.000113	0.1786	0.000165
1.948	0.1838	0.000128	0.1834	0.000186
2.092	0.1896	0.000108	0.1892	0.000157
2.292	0.1958	0.000137	0.1955	0.000200
2.492	0.1996	0.000173	0.1994	0.000252
2.693	0.2017	0.000217	0.2014	0.000317
2.893	0.2020	0.000270	0.2008	0.000395
3.093	0.2032	0.000399	0.2024	0.000582
3.335	0.2004	0.000438	0.2013	0.000639
3.676	0.1950	0.000550	0.1936	0.000802
4.117	0.1869	0.000752	0.1837	0.001096
4.582	0.1756	0.001238	0.1738	0.001803
5.026	0.1692	0.001542	0.1596	0.002249
5.442	0.1554	0.002610	0.1490	0.003803
5.959	0.1556	0.002151	0.1461	0.003132
6.682	0.1596	0.003502	0.1391	0.005114

Table 9: v_2 of charged hadrons as a function of p_T. The measurements are performed with respect to the combined **RXN and MPC event planes for 40-60% central collisions**.

$p_T(GeV/c)$	$v_2(RXN)$	$\sigma_{stat}(v_2)$	$v_2(MPC)$	$\sigma_{stat}(v_2)$
0.425	0.0586	0.000067	0.0603	0.000104
0.475	0.0660	0.000070	0.0678	0.000109
0.525	0.0736	0.000073	0.0748	0.000114
0.575	0.0805	0.000077	0.0820	0.000121
0.624	0.0876	0.000081	0.0889	0.000128
0.674	0.0941	0.000086	0.0953	0.000136
0.724	0.1007	0.000092	0.1016	0.000144
0.775	0.1067	0.000097	0.1075	0.000153
0.824	0.1126	0.000104	0.1136	0.000162
0.874	0.1184	0.000110	0.1192	0.000173
0.924	0.1241	0.000117	0.1245	0.000184
0.974	0.1294	0.000125	0.1298	0.000195
1.048	0.1369	0.000096	0.1375	0.000151
1.148	0.1471	0.000108	0.1472	0.000170
1.248	0.1563	0.000122	0.1559	0.000192
1.348	0.1651	0.000138	0.1651	0.000217
1.448	0.1735	0.000156	0.1733	0.000246
1.548	0.1810	0.000178	0.1802	0.000279
1.648	0.1875	0.000201	0.1869	0.000316
1.748	0.1935	0.000227	0.1924	0.000357
1.848	0.1988	0.000256	0.1977	0.000403
1.948	0.2032	0.000289	0.2015	0.000455
2.092	0.2086	0.000243	0.2072	0.000383
2.292	0.2137	0.000308	0.2113	0.000485
2.492	0.2165	0.000387	0.2145	0.000610
2.693	0.2173	0.000483	0.2144	0.000762
2.893	0.2169	0.000599	0.2121	0.000944
3.093	0.2182	0.000885	0.2122	0.001395
3.335	0.2137	0.000965	0.2099	0.001520
3.676	0.2086	0.001201	0.2028	0.001892
4.117	0.2038	0.001625	0.1923	0.002561
4.582	0.1910	0.002655	0.1775	0.004176
5.026	0.1895	0.003302	0.1675	0.005201
5.442	0.1790	0.005564	0.1710	0.008788
5.957	0.1790	0.004609	0.1628	0.007259
6.680	0.2025	0.007569	0.1628	0.011890

Table 10: v_2 of charged hadrons as a function of p_T. The measurements are performed with respect to the combined **RXN and MPC event planes for 0-20% central collisions**.

$p_T(GeV/c)$	$v_2(RXN)$	$\sigma_{stat}(v_2)$	$v_2(MPC)$	$\sigma_{stat}(v_2)$
0.425	0.0244	0.000029	0.0249	0.000044
0.475	0.0277	0.000030	0.0282	0.000046
0.525	0.0310	0.000031	0.0315	0.000048
0.575	0.0342	0.000033	0.0347	0.000051
0.624	0.0374	0.000035	0.0378	0.000054
0.675	0.0404	0.000037	0.0408	0.000057
0.724	0.0434	0.000040	0.0438	0.000061
0.775	0.0463	0.000042	0.0468	0.000064
0.824	0.0490	0.000044	0.0495	0.000068
0.875	0.0516	0.000047	0.0521	0.000073
0.925	0.0543	0.000050	0.0550	0.000077
0.975	0.0568	0.000053	0.0575	0.000082
1.048	0.0605	0.000041	0.0613	0.000063
1.148	0.0654	0.000046	0.0662	0.000070
1.248	0.0702	0.000052	0.0713	0.000079
1.348	0.0750	0.000058	0.0761	0.000089
1.448	0.0796	0.000065	0.0810	0.000100
1.548	0.0842	0.000074	0.0857	0.000114
1.648	0.0882	0.000084	0.0897	0.000129
1.748	0.0921	0.000095	0.0942	0.000146
1.848	0.0957	0.000107	0.0980	0.000165
1.948	0.0992	0.000122	0.1018	0.000187
2.092	0.1033	0.000103	0.1066	0.000159
2.292	0.1081	0.000132	0.1119	0.000204
2.492	0.1118	0.000169	0.1163	0.000260
2.692	0.1143	0.000214	0.1199	0.000329
2.892	0.1152	0.000270	0.1206	0.000415
3.334	0.1166	0.000439	0.1239	0.000675
3.675	0.1129	0.000562	0.1217	0.000863
4.117	0.1063	0.000781	0.1160	0.001200
4.583	0.0998	0.001298	0.1068	0.001992
5.029	0.0953	0.001615	0.1009	0.002482
5.444	0.0904	0.002698	0.0957	0.004142
5.968	0.0851	0.002192	0.0867	0.003364
6.686	0.0848	0.003477	0.0921	0.005350

Table 11: v_2 of charged hadrons as a function of p_T. The measurements are performed with respect to the combined **RXN and MPC event planes for 20-40% central collisions**.

$p_T(GeV/c)$	$v_2(RXN)$	$\sigma_{stat}(v_2)$	$v_2(MPC)$	$\sigma_{stat}(v_2)$
0.425	0.0491	0.000034	0.0497	0.000048
0.475	0.0551	0.000036	0.0558	0.000050
0.525	0.0612	0.000037	0.0617	0.000053
0.575	0.0672	0.000039	0.0676	0.000056
0.625	0.0728	0.000041	0.0732	0.000059
0.675	0.0784	0.000044	0.0787	0.000062
0.724	0.0836	0.000047	0.0839	0.000066
0.775	0.0887	0.000049	0.0890	0.000070
0.824	0.0935	0.000052	0.0938	0.000074
0.875	0.0984	0.000056	0.0986	0.000079
0.925	0.1031	0.000059	0.1033	0.000084
0.975	0.1077	0.000062	0.1079	0.000089
1.048	0.1142	0.000048	0.1143	0.000068
1.148	0.1228	0.000054	0.1229	0.000077
1.248	0.1311	0.000061	0.1313	0.000086
1.348	0.1391	0.000068	0.1392	0.000097
1.448	0.1468	0.000077	0.1470	0.000109
1.548	0.1539	0.000087	0.1542	0.000124
1.648	0.1605	0.000098	0.1609	0.000140
1.748	0.1668	0.000111	0.1671	0.000158
1.848	0.1724	0.000125	0.1726	0.000178
1.948	0.1774	0.000141	0.1777	0.000201
2.092	0.1833	0.000119	0.1836	0.000170
2.292	0.1899	0.000152	0.1906	0.000216
2.492	0.1941	0.000192	0.1948	0.000273
2.692	0.1966	0.000241	0.1975	0.000343
2.893	0.1973	0.000301	0.1977	0.000429
3.335	0.1964	0.000488	0.1992	0.000696
3.675	0.1911	0.000616	0.1916	0.000878
4.116	0.1820	0.000846	0.1823	0.001205
4.582	0.1713	0.001398	0.1742	0.001989
5.026	0.1632	0.001742	0.1586	0.002482
5.443	0.1482	0.002955	0.1434	0.004199
5.960	0.1484	0.002429	0.1420	0.003454
6.682	0.1455	0.003941	0.1326	0.005631

References

[1] A. Taranenko et al., PHENIX AN760, "Measurements of elliptic and hexadecapole flow of charged hadrons in Au+Au collisions at 200 GeV" , 2009

[2] J. Adams *et al.* [STAR Collaboration], "Azimuthal anisotropy in Au + Au collisions at 200-GeV," Phys. Rev. C **72**, 014904 (2005)
Data points: http://drupal.star.bnl.gov/STAR/files/starpublications/48/data.html

[3] J. Adams *et al.* [STAR Collaboration], "Azimuthal anisotropy and correlations at large transverse momenta in p + p and Au + Au collisions at 200-GeV," Phys. Rev. Lett. **93**, 252301 (2004)
Data points: http://drupal.star.bnl.gov/STAR/files/starpublications/45/data.html

[4] B. I. Abelev *et al.* [STAR Collaboration], "Centrality dependence of charged hadron and strange hadron elliptic flow from $\sqrt{s_{NN}}$ = 200 GeV Au+Au collisions," Phys. Rev. C **77**, 054901 (2008)
Data points:http://drupal.star.bnl.gov/STAR/files/starpublications/108/data.html

[5] B. B. Back *et al.* [PHOBOS Collaboration], "Centrality and pseudorapidity dependence of elliptic flow for charged hadrons in Au + Au collisions at $\sqrt{s_{NN}}$ = 200-GeV," Phys. Rev. C **72**, 051901 (2005), Data points:
http://www.phobos.bnl.gov/Publications/Physics/Flow_v2_cent_pt/final_ascii_table.txt

[6] B.B. Back et al . (PHOBOS Collaboration), Phys. Rev. Lett. **94**, 122303 (2005).

[7] A. Adare *et al.* [PHENIX Collaboration], "Scaling properties of azimuthal anisotropy in Au + Au and Cu + Cu collisions at $\sqrt{s_{NN}}$ = 200-GeV," Phys. Rev. Lett. **98**, 162301 (2007)

[8] S. Afanasiev *et al.* [PHENIX Collaboration], "Systematic Studies of Elliptic Flow Measurements in Au+Au Collisions at $\sqrt{s_{NN}}$ = 200-GeV," Phys. Rev. C **80**, 024909 (2009)

[9] S. A. Voloshin, A. M. Poskanzer and R. Snellings, arXiv:0809.2949 [nucl-ex].

[10] Eric Richardson, Event plane QA
www.phenix.bnl.gov/WWW/p/draft/erichard/flow_analysis/WebPage/QA/QA.html

[11] J. Jia [PHENIX Collaboration], "Ways to constrain the away side jet in Au + Au collisions in PHENIX," Nucl. Phys. A **783**, 501 (2007)

[12] B. Alver *et al.* [PHOBOS Collaboration], "Elliptic flow and initial eccentricity in Cu + Cu and Au + Au collisions at RHIC," J. Phys. G **34**, S887 (2007) [arXiv:nucl-ex/0701054].